Supporting Information

Unravelling the Underlying Mechanism of the Reduction of Aldehydes/Ketones with Metal Borohydride in an Aprotic Solvent

Xinying Li,[a] Kang-Jia Xin,[b] Shasha Liang,[a] Xi-Hong Long,[a] Yan-Na Ma,*[a] Xuenian Chen*[a,b]

[a] College of Chemistry, Zhengzhou University, Zhengzhou, 450001, China.
[b] School of Chemistry and Chemical Engineering, Henan Key Laboratory of Boron Chemistry and Advanced Energy Materials, Henan Normal University, Xinxiang, 453007, China.
E-mail: Xuenian_Chen@zzu.edu.cn; mayanna@zzu.edu.cn.

Contents

1. General methods and materials

Allof the reactions and manipulations were carried out under nitrogen with the use of standard inert atmosphere and Schlenk technique unless otherwise indicated. All reagents were purchased from commercial sources and used without further treatment, except the liquid substrates which were dried over 4 Å molecular sieves prior to use. All solvents were purified according to literature procedures and stored under nitrogen. The ^{1}H NMR spectra was recorded on a Bruker advance III 400 spectrometer in $CDCl_3$ with TMS as internal standard. Chemical shifts (δ) were measured in ppm with TMS (δ = 0) for ^{1}H as internal standard. All reactions were monitored by ^{11}B NMR. The ^{11}B NMR spectra were recorded using a 128 MHz spectrometer and externally referenced to $BF_3{\cdot}OEt_2$ in C_6D_6 (δ = 0.00 ppm).

2. The average local ionization energy (ALIE)

The average local ionization energy (ALIE, $\bar{I}(\mathbf{r})$) is rigorously defined within the framework of self-consistent-filed molecular orbital (SCF-MO) theory, as given by eq. (1):

$$\bar{I}(\mathbf{r}) = -\sum_{i=1}^{\mathrm{HOMO}} \frac{\varepsilon_i \rho_i(\mathbf{r})}{\rho(\mathbf{r})} \qquad (1)$$

$\rho_i(\mathbf{r})$ is the electronic density of ith molecular orbital at the point $\mathbf{r}$, ε_i is the eigenvalue of the orbital energy, and $\rho(\mathbf{r})$ is the total electron density. The smaller the ALIE minima is, the more nucleophilicity the specie is. The ALIE analysis is performed by using Multiwfn software package.[1] Based on this method, the isosurfaces of average local ionization energy (ALIE) of THF, Et_3N, CH_3O^-, $CH_3CH_2O^-$, $^{i}PrO^-$ and $^{t}BuO^-$ (ρ = 0.005 a.u.) were calculated as shown in Figure S1.

3. Experimental Section:

3.1 The reduction with $M(BH_4)_n$ (M = Li, Na, Ca)

3.1.1 The reaction of $LiBH_4$ and cinnamaldehyde in THF

In a glovebox, $LiBH_4$ (2 mmol) was put into a 50 mL Schlenk flask and then connected to a Schlenk line. 20 mL THF was injected into the flask. The reactions mixture was stirred at room temperature. Then different amounts of Et_3N (x mmol, x = 0, 2, 4, 6, 8, 10, 15, 20) were added to the solution, followed by 10 mmol cinnamaldehyde. The reaction was monitored by ^{11}B NMR. When $LiBH_4$ was completely consumed based on the NMR, the reaction was quenched with 0.2 mL deionized water. The solvent was removed and $CDCl_3$ was added to record an NMR spectrum. Yields were calculated based upon the integrated values of the characteristic signals in ^1H and $^1H\{^{11}B\}$ NMR (Figures 2, S2, and S18-S25).

3.1.2 The reaction of $LiBH_4$ and 4-fluorophenylacetone in THF

In a glovebox, $LiBH_4$ (2 mmol) was put into a 50 mL Schlenk flask and then connected to a Schlenk line. 20 mL THF was injected into the flask. The reactions mixture was stirred at room temperature. Then different amounts of Et_3N (x mmol, x = 0, 2, 4, 6, 8, 10, 15, 20) were added to the solution, followed by 10 mmol 4-fluorophenylacetone. The reaction was monitored by ^{11}B NMR. When $LiBH_4$ was completely consumed based on the NMR, the reaction was quenched with 0.2 mL deionized water. The solvent was removed and $CDCl_3$ was added to record an NMR spectrum. Yields were calculated based upon the integrated values of the characteristic signals in ^1H and $^1H\{^{11}B\}$ NMR (Figures S3, S4, and S26-S33).

3.1.3 The reaction of $Ca(BH_4)_2$ and cinnamaldehyde in THF

By a similar procedure of 3.1.1, in which $LiBH_4$ was replaced by $Ca(BH_4)_2$, the reaction of $Ca(BH_4)_2$ and cinnamaldehyde in THF was examined and the results showed in Figures S9 and S34-41.

3.1.4 The reaction of $Ca(BH_4)_2$ and 4-fluorophenylacetone in THF

By a similar procedure of 3.1.2, in which $LiBH_4$ was replaced by $Ca(BH_4)_2$, the reaction of $Ca(BH_4)_2$ and 4-fluorophenylacetone in THF was examined and the results showed in Figures S10 and S42-49.

3.1.5 The reaction of $NaBH_4$ and cinnamaldehyde in THF

By a similar procedure of 3.1.1, in which $LiBH_4$ was replaced by $NaBH_4$, the reaction of $NaBH_4$

and cinnamaldehyde in THF was examined and the results showed in Figure S11.

3.1.6 The reaction of $NaBH_4$ and 4-fluorophenylacetone in THF

By a similar procedure of 3.1.2, in which $LiBH_4$ was replaced by $NaBH_4$, the reaction of $NaBH_4$ and 4-fluorophenylacetone in THF was examined and the results showed in Figure S11.

3.1.7 The reaction of $LiBH_4$ and cinnamaldehyde in DME

By a similar procedure of 3.1.1, in which THF was replaced by DME, the reaction of $LiBH_4$ and cinnamaldehyde in DME was examined and the results showed in Figure 3 and S50-S57.

3.1.8 The reaction of $LiBH_4$ and 4-fluorophenylacetone in DME

By a similar procedure of 3.1.2, in which THF was replaced by DME, the reaction of $LiBH_4$ and 4-fluorophenylacetone in DME was examined and the results showed in Figure S3 and S58-S65.

3.2 Capture the THF·BH_3 at -40℃

In a glovebox, $NaBH_4$ (1 mmol) was put into a 25 mL Schlenk flask. 10 mL THF was injected into the flask and the mixture was stirred. 0.5 mL of the above solution was taken into a nuclear magnetic tube which was kept in -78℃ for 10 min. 0.25 mmol CH_3CHO (in THF) was quickly added. Then the NMR tube was rapidly put in the NMR instrument which was set up at -40℃ previously. The whole reaction process was monitored by ^{11}B and $^{11}B\{^1H\}$ NMR spectra at -40℃ (Figure S5).

3.3 The detection of 3-phenyl-1-propanol

In a glovebox, $NaBH_4$ (2 mmol) was put into a 50 mL Schlenk flask which was connected to a Schlenk line. 20 mL DME was injected into the flask. The reactions mixture was stirred at room temperature. 10 mmol cinnamaldehyde was added and the reaction was monitored by ^{11}B NMR. When $NaBH_4$ was completely consumed based on NMR, the reaction was quenched with 0.2 mL deionized water. The solvent was removed and $CDCl_3$ was added to record a ^1H NMR spectrum (Figure S6).

3.4 The reaction of THF·BH_3 with sodium alkoxide

In a glovebox, sodium *tert*-butoxide (1 mmol) was put into a 10 mL Schlenk flask which was connected to a Schlenk line. 1 mL THF·BH_3 (1M) was injected into the flask. The reactions mixture was stirred at room temperature and monitored by ^{11}B NMR spectroscopy. After 5 min, the ^{11}B NMR spectrum of the reaction mixture is shown in Figure S7.

3.5 The reaction of MBH_4 (M = Li, Na) with cinnamaldehyde in the presence of Et_3N in isopropanol

In a glovebox, MBH_4 (M = Li, Na, 2 mmol) was put into a 50 mL Schlenk flask which was then connected to a Schlenk line. 20 mL isopropanol was injected into the flask. The reactions mixture was stirred at room temperature. 20 mmol Et_3N were added to the solution, followed by 10 mmol cinnamaldehyde. The reaction was monitored by ^{11}B NMR. When MBH_4 was completely consumed based on NMR, the reaction was quenched with 0.2 mL deionized water. The solvent was removed and $CDCl_3$ was added to record an $^1H\{^{11}B\}$ NMR spectrum (Figure S8).

3.6 The role of Li^+ in the reduction of cinnamaldehyde with $THF{\cdot}BH_3$ in THF

In a glovebox, lithium chloride (1 mmol) was put into a 25 mL Schlenk flask which was then connected to a Schlenk line. 9 mL THF and 1 mL $THF{\cdot}BH_3$ (1 M) was injected into the flask. The reactions mixture was stirred at room temperature. 5 mmol cinnamaldehyde was added to the solution. After 15 min, the reaction was quenched with 0.2 mL deionized water. The solvent was removed and $CDCl_3$ was added to record a ^1H NMR spectrum based on which the yields were calculated (Table S1 and Figure S12).

By a similar procedure, using lithium *tert*-butoxide (1 mmol) replaced lithium chloride (1 mmol). The ^1H NMR spectrum was recorded (Figure S13) based on which the yields were calculated (Table S1 and Figure S13).

By a similar procedure, lithium salts were not used in the reaction as a control experiment. The ^1H NMR spectrum was recorded (Figure S14) based on which the yields were calculated (Table S1 and Figure S14).

3.7 The reaction of Et_3NBH_3 with cinnamaldehyde in THF

A 50 mL Schlenk flask was connected to a Schlenk line, and 20 mL THF, 2 mmol Et_3NBH_3, 8 mmol cinnamaldehyde were added in sequence. The reactions mixture was stirred at room temperature. At different time intervals (1d, 2d, 3d), 1 mL samples were withdrawn. After removing the solvent, $CDCl_3$ was added to record a ^1H NMR spectrum(S16).

4. Discussion

4.1 The disproportionation of $[BH_3OCHR_1R_2]^-$

When the first hydride of the BH_4^- anion was transferred to the C atom of the carbonyl group, an alkoxyl anion and a BH_3 group were formed at the same time. BH_3 coordinated with a THF solvent molecule to form THF·BH_3. We speculate that the alkoxyl anion formed here could replace THF to form alkoxyl anion-coordinated borane (alkoxyborohydridoborates, $BH_3OCHR_1R_2^-$) because of the high nucleophilicity of the alkoxyl anion (Fig. S1, detailed inofrmation see ESI†). To prove this hypothesis, we set up a reaction of THF·BH_3 and NaO^{t}Bu at a 1:1 ratio in THF with the desirable product being $NaBH_3(O^tBu)$. However, the signals of $B(O^tBu)_4^-$, $BH(O^tBu)_3^-$, $BH_2(O^tBu)_2^-$, and $BH_3(O^tBu)^-$ were observed in the ^{11}B NMR spectra (see Figure S7), indicating the formation of $BH_3(O^tBu)^-$, followed by conversion to other alkoxyl-coordinated borane complexes step-by-step through the disproportionation (eqn (1)-(3)).[2, 3]

$$2\ BH_3(O^tBu)^- \rightarrow BH_4^- + BH_2(O^tBu)_2^- \quad (1)$$

$$2\ BH_2(O^tBu)_2^- \rightarrow BH_3(O^tBu)^- + BH(O^tBu)_3^- \quad (2)$$

$$2\ BH(O^tBu)_3^- \rightarrow BH_2(O^tBu)_2^- + B(O^tBu)_4^- \quad (3)$$

It is worth noting that the similar disproportionation process of $BH_3(OR)^-$ has been proposed in protic solvents,[2] but the reactions in the protic and aprotic solvents are essentially different. In an aprotic solvent such as THF, a THF·BH_3 intermediate was formed first and then converted into the alkoxyl anion coordinated borane complex (BH_3OR^-). However, in a protic solvent, the alkoxyl anion coordinated borane complex (BH_3OR^-) was directly formed in the initial step, which then rapidly transpires into a disproportionation reaction. To confirm this difference, we changed the solvent in the template experiment to isopropyl alcohol, in which $Et_3N{\cdot}BH_3$ could hardly be observed in the NMR even if ten equiv. of Et_3N was added (Figure S8a), and almost eight mmol aldehyde was consumed. A similar result was obtained when $LiBH_4$ was used instead of $NaBH_4$ (Figure S8b). These results indicate that the reduction mechanisms of aldehydes/ketones with $NaBH_4$ or $LiBH_4$ in aprotic solvents are different from those in protic solvents, and the formation of the solvent molecule coordinated borane, L·BH_3, is a remarkable feature for this mechanism.

4.2 Solvents participation in the reaction

To explore the impact of solvents on the reaction, we selected DME as a solvent for the comparison with THF. When these reactions were carried out in DME, the reduced cinnamyl alcohol product obviously decreased by comparison with that in THF when 1-4 equiv. of Et_3N were used (Figure S15). That is reasonable because the formed BH_3 group will rapidly coordinate with the THF solvent to form the $THF{\cdot}BH_3$ complex when the reaction is in THF. On the contrary, when the reaction is in DME, the formed BH_3 group self-dimerizes to form B_2H_6 because BH_3 does not coordinate with DME.[4] In general, the formed BH_3 coordinates more rapidly with Et_3N, so only 2 mmol aldehyde was reduced. However, the formed $THF{\cdot}BH_3$ can continue to the reduction of aldehyde during the exchange of ligands of THF and Et_3N if the reaction is carried out in THF. Only when excess Et_3N is added to the reaction, the formed BH_3 could be captured completely (Figure S15). Thus, it is obvious that the coordinating ability of solvents influences the reaction.

5.Suplementary Figures and NMR spectra

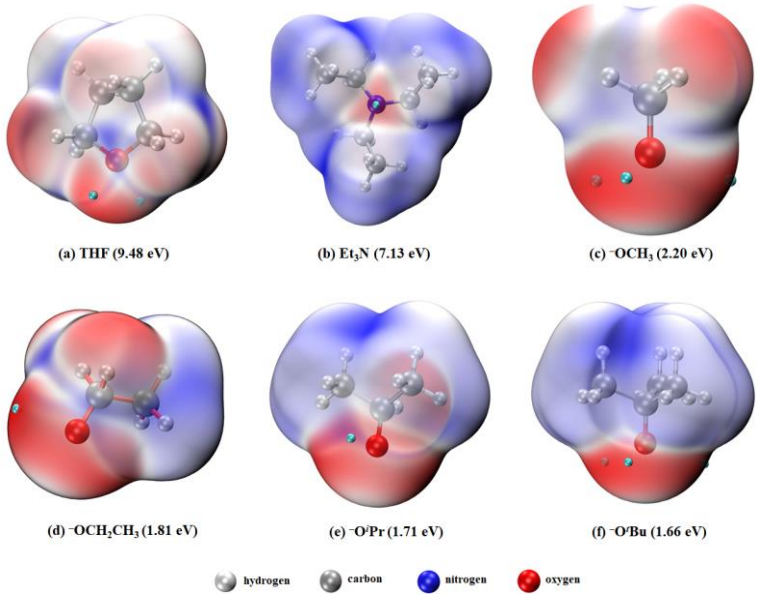

Figure S1. The isosurfaces of calculated average local ionization energy (ALIE) of THF, Et_3N, CH_3O^-, $CH_3CH_2O^-$, $^iPrO^-$ and $^tBuO^-$ ($\rho = 0.005$ a.u.). Red spheres indicate the position of minima of ALIE on this surface and the ALIE minima are indicated in parentheses.

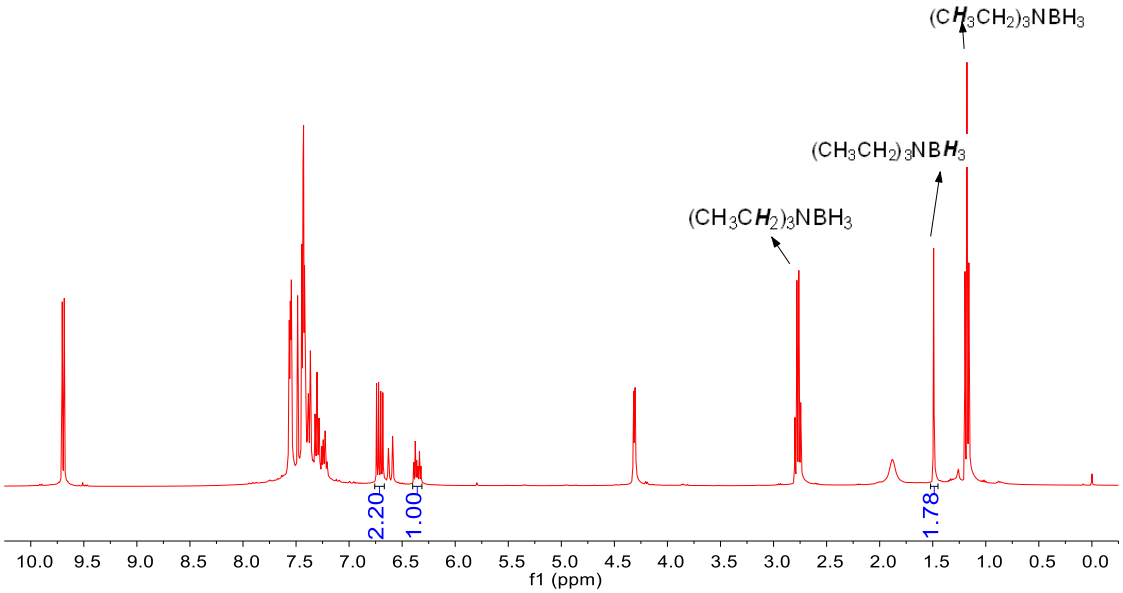

Figure S2. $^1H\{^{11}B\}$ NMR spectra in $CDCl_3$ for the reaction of cinnamaldehyde, $LiBH_4$ and Et_3N at a ratio of 10 : 2 : 6 in THF.

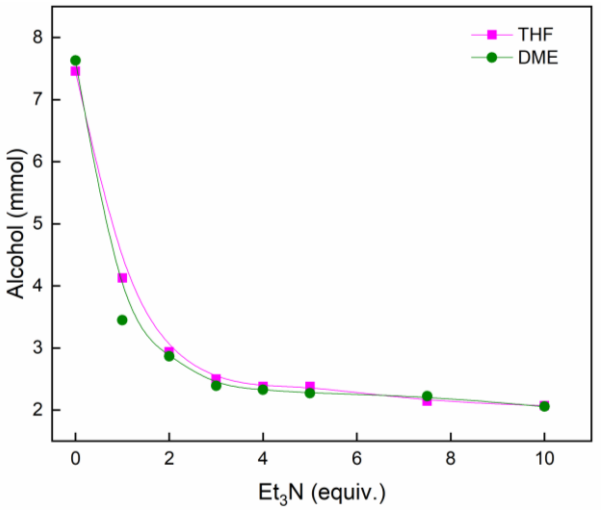

Figure S3. The reactions of $LiBH_4$ with 4-fluorophenylacetone in THF and DME at room temperature.

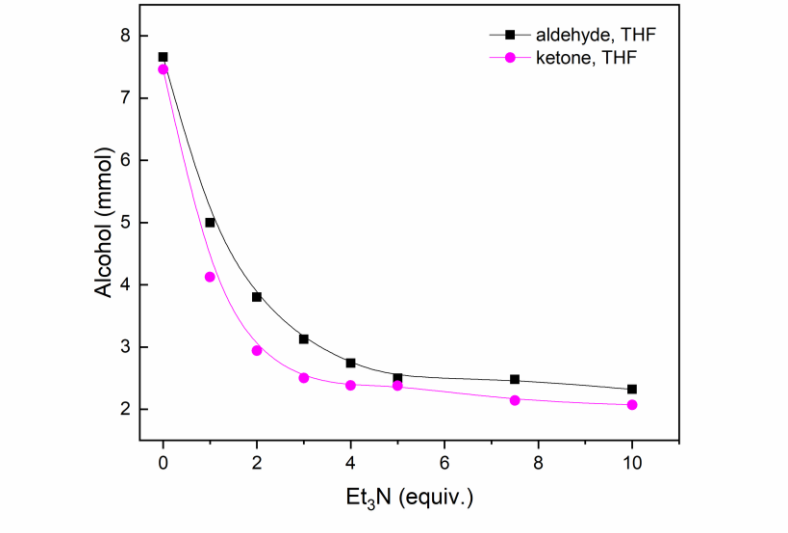

Figure S4. The reaction of $LiBH_4$ with aldehyde and ketone in THF at room temperature.

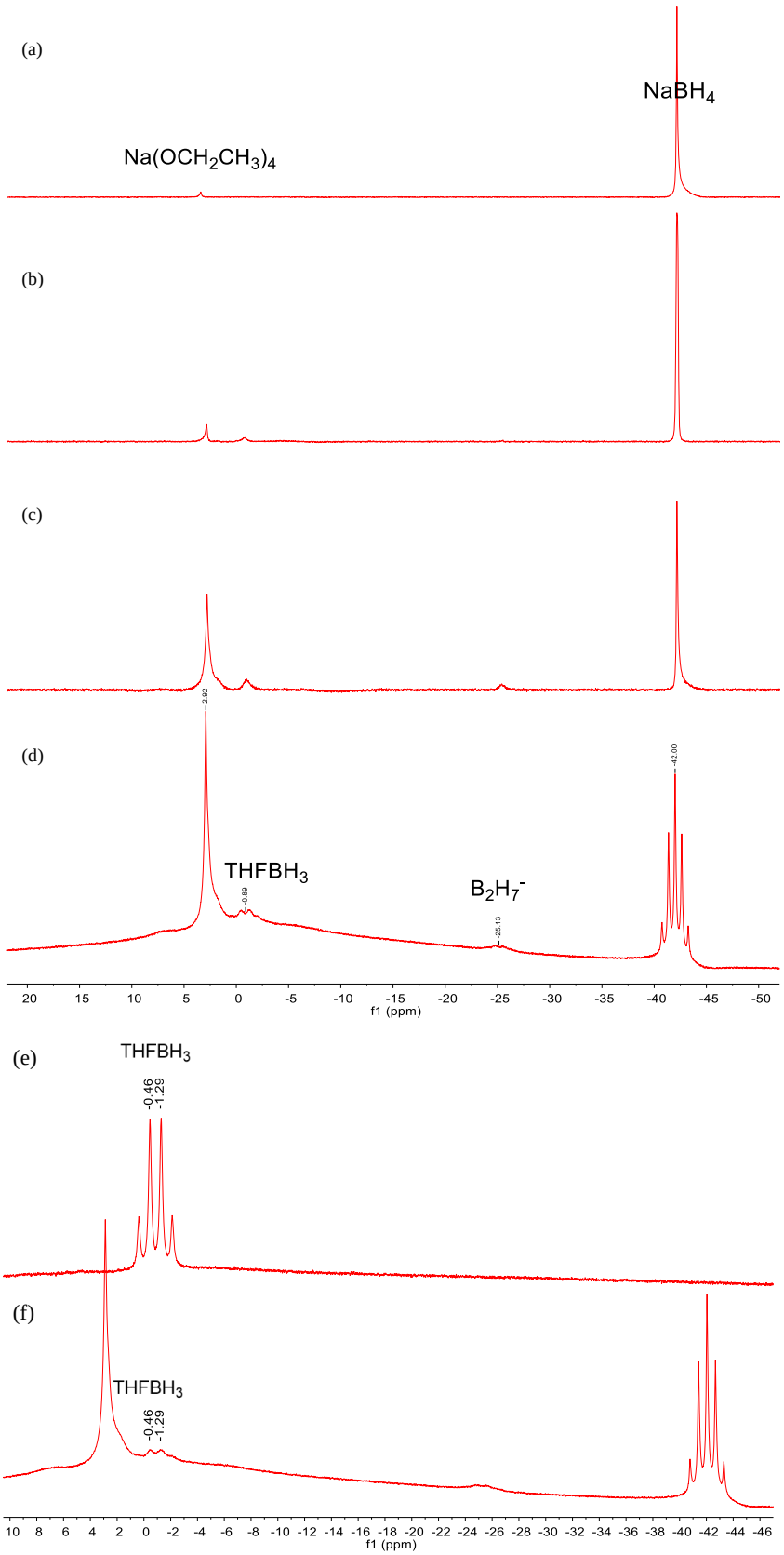

Figure S5. $^{11}B\{^{1}H\}$ NMR spectra for the reaction of $NaBH_4$ with acetaldehyde in THF without Et_3N at -40 °C (a) 5 min, (b) 10 min, (c) 15 min, (d, f) ^{11}B NMR spectra of c and (e) pure $THFBH_3$.

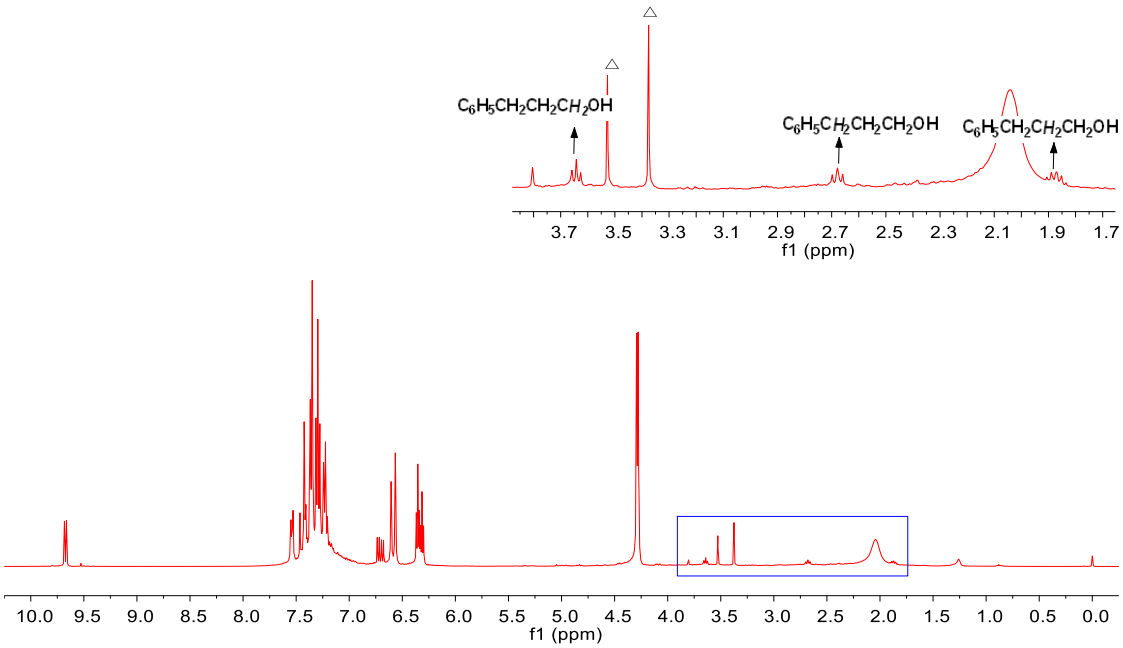

Figure S6. ^{1}H NMR spectra in $CDCl_3$ for the reaction of $NaBH_4$ with cinnamaldehyde in DME without Et_3N, enlarged view of part in blue box (insert) (△stands for solvent, DME).

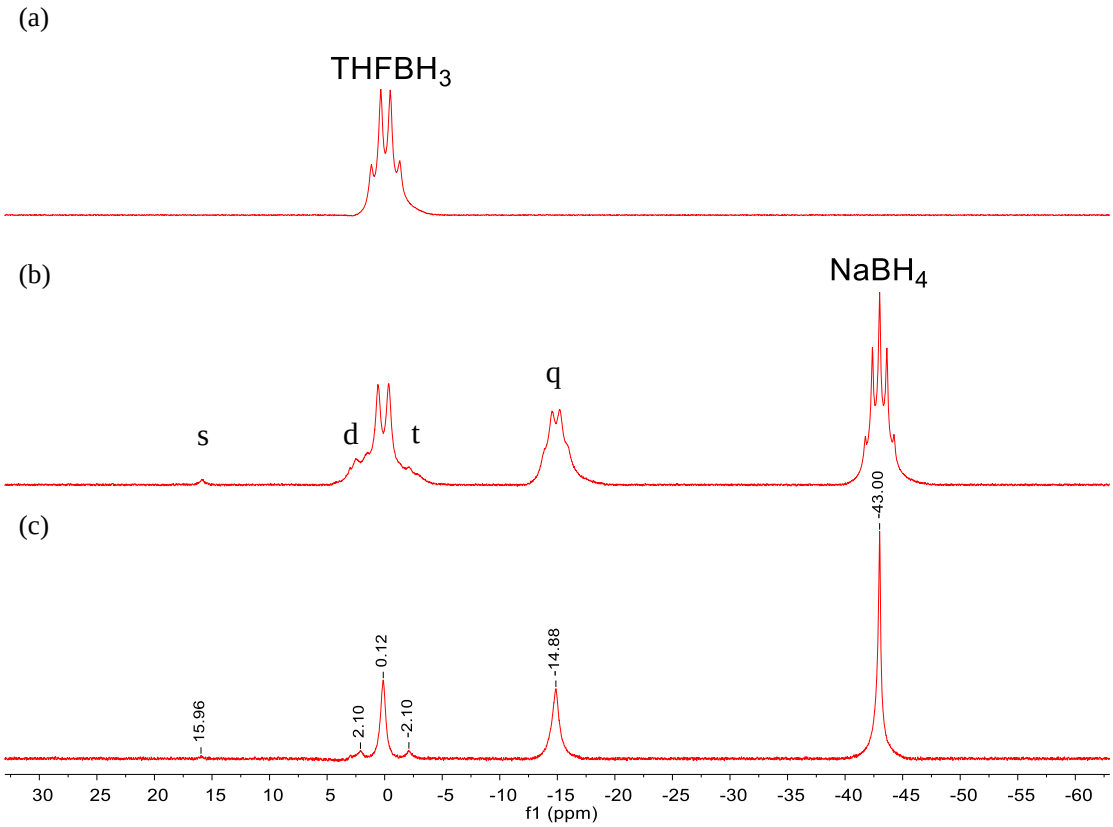

Figure S7. ^{11}B NMR spectra for (a) $THFBH_3$; (b) the reaction of $THFBH_3$ with sodium *tert*-butoxide in THF at room temperature; (c) $^{11}B\{^1H\}$ NMR spectra of b.

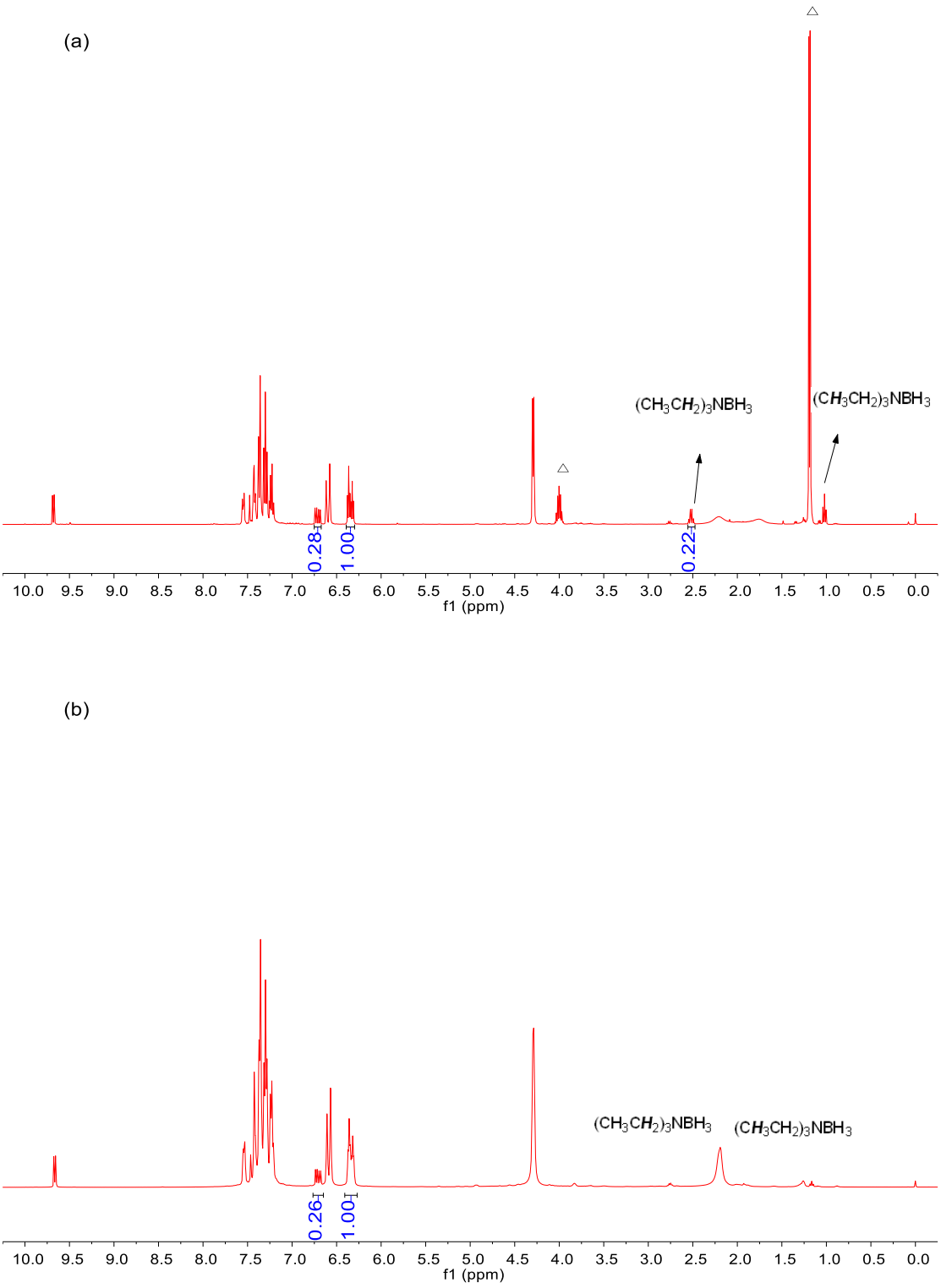

Figure S8. $^{1}H\{^{11}B\}$ NMR spectra in $CDCl_3$ for the reaction of $NaBH_4$ (a) and $LiBH_4$ (b) with cinnamaldehyde in isopropanol (△stands for solvent, isopropanol).

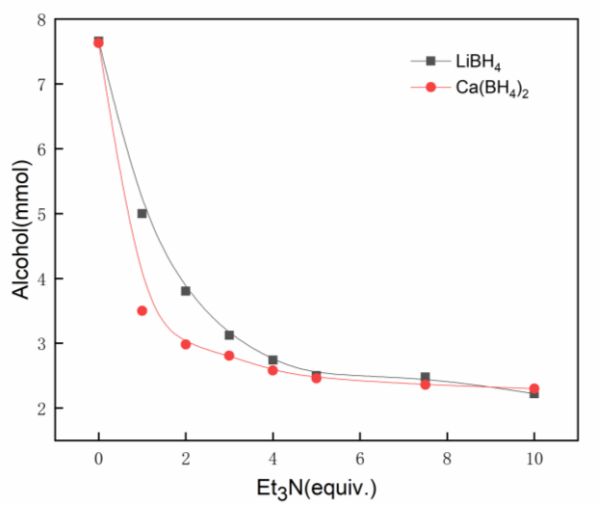

Figure S9. The reaction of $LiBH_4$ and $Ca(BH_4)_2$ with aldehyde and different equivalents of Et_3N in THF.

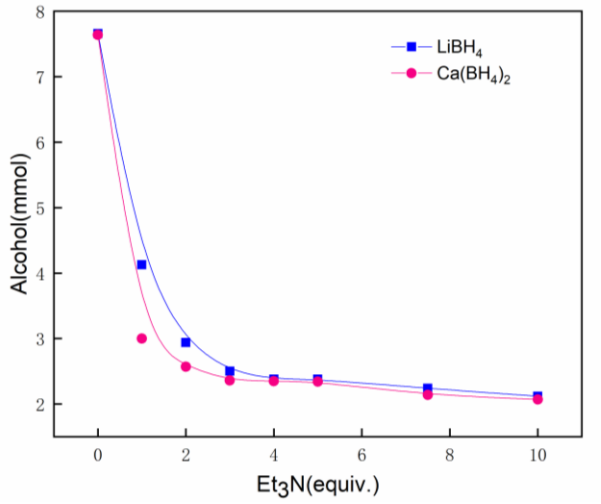

Figure S10. The reaction of $LiBH_4$ and $Ca(BH_4)_2$ with ketone and different equivalents of Et_3N in THF.

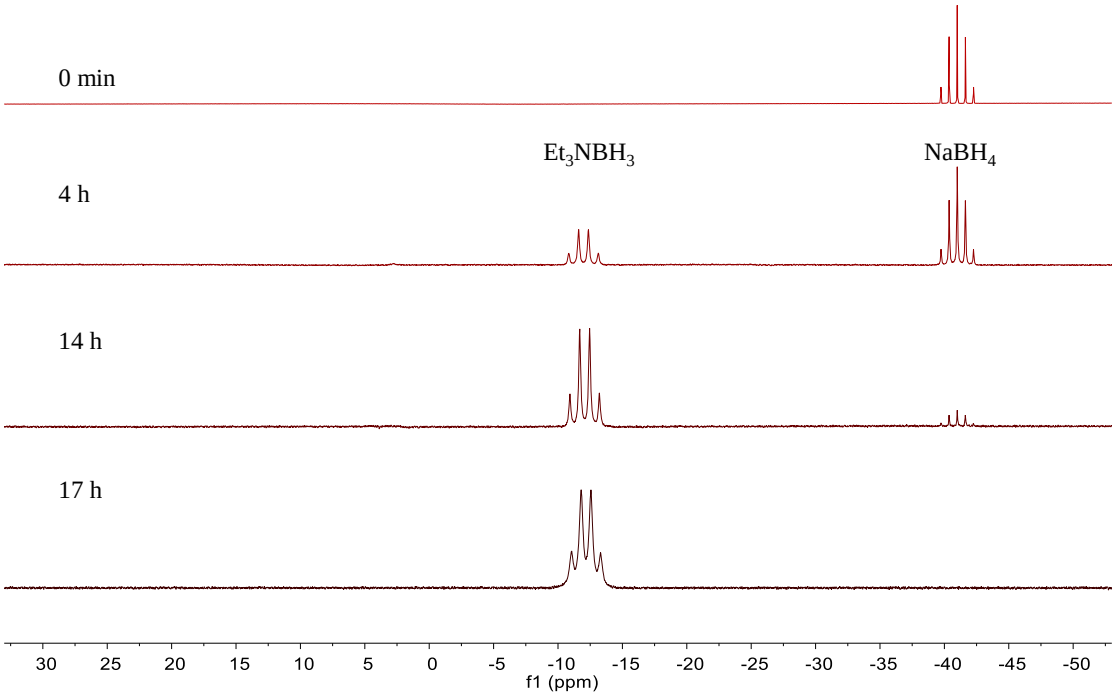

Figure S11. ^{11}B NMR spectra for the reaction of cinnamaldehyde, $NaBH_4$, Et_3N at a ratio of 10 : 2 : 5 in THF at different time.

Table S1 The reactions of THF·BH_3 and cinnamaldehyde with and without additive for 15 min.[a]

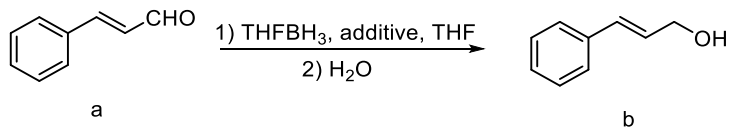

a b

Entry	additive	a (mmol)	b (mmol)
1	none	2.82	2.17
2	LiCl	2.38	2.61
3	^{t}BuOLi	2.03	2.96

[a] Yields were determined by ^{1}H NMR spectroscopy.

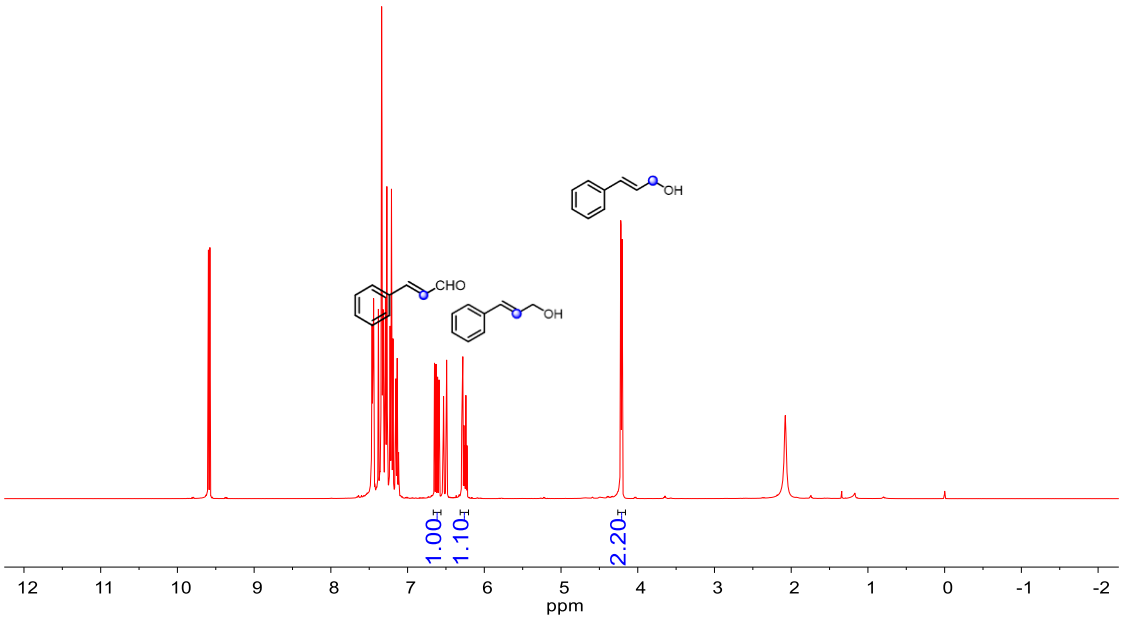

Figure S12. ^{1}H NMR spectra in $CDCl_3$ for the reaction of THF·BH_3 and cinnamaldehyde with LiCl in THF for 15 min.

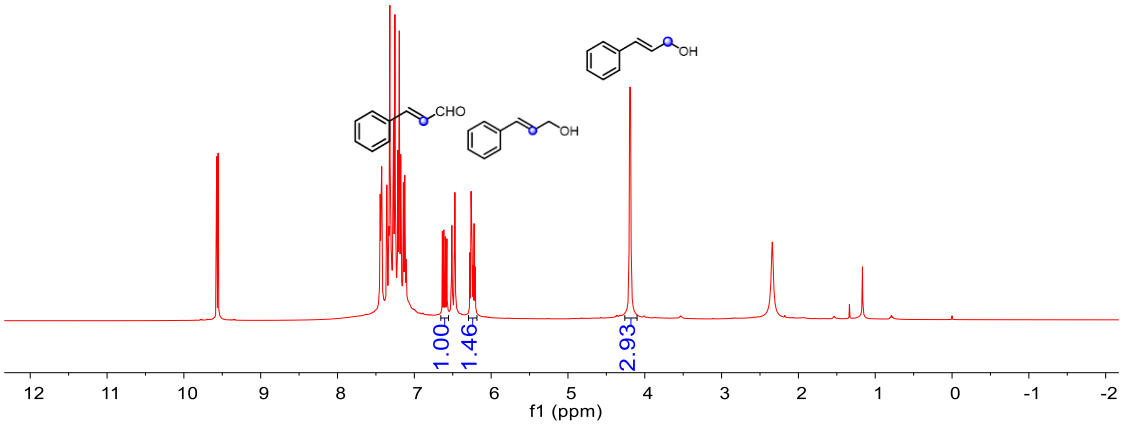

Figure S13. ^{1}H NMR spectra in $CDCl_3$ for the reaction of $THF{\cdot}BH_3$ and cinnamaldehyde with $^{t}BuOLi$ in THF for 15 min.

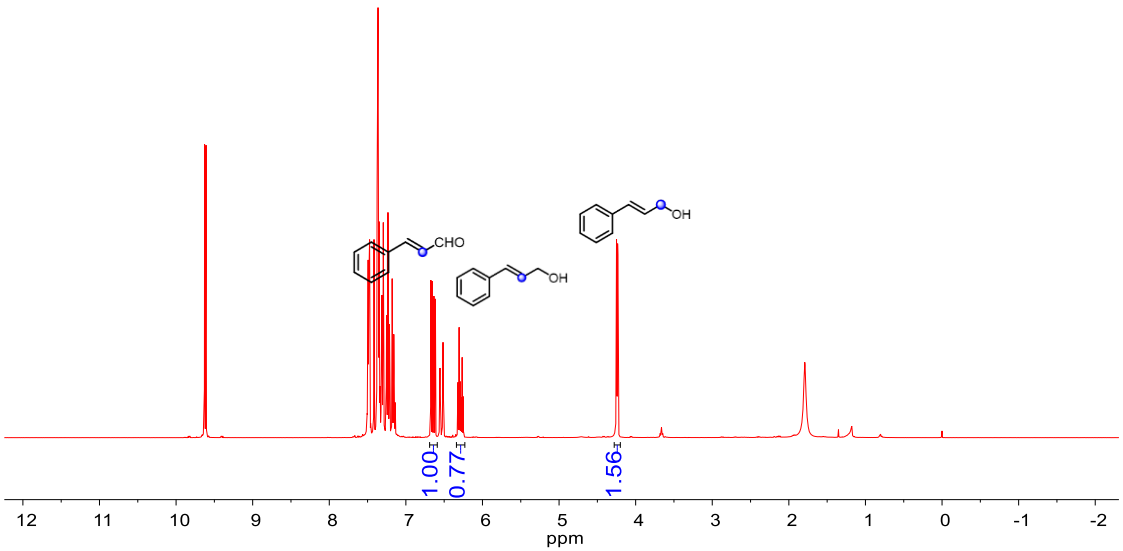

Figure S14. ^{1}H NMR spectra in $CDCl_3$ for the reaction of $THF{\cdot}BH_3$ and cinnamaldehyde without additive in THF for 15 min.

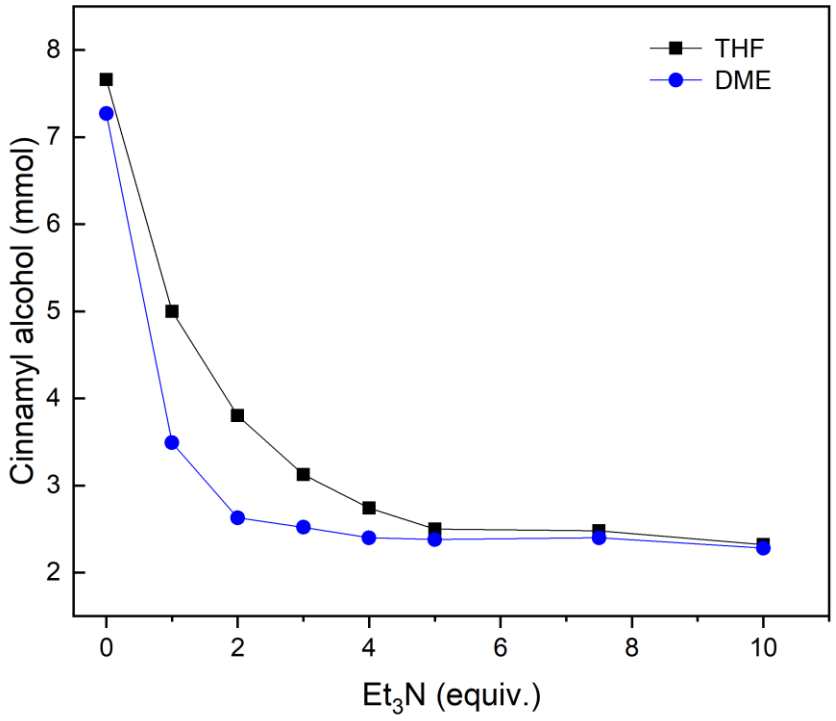

Figure S15. The reactions of $LiBH_4$ with cinnamaldehyde and different equivalents of Et_3N in THF and DME at room temperature.

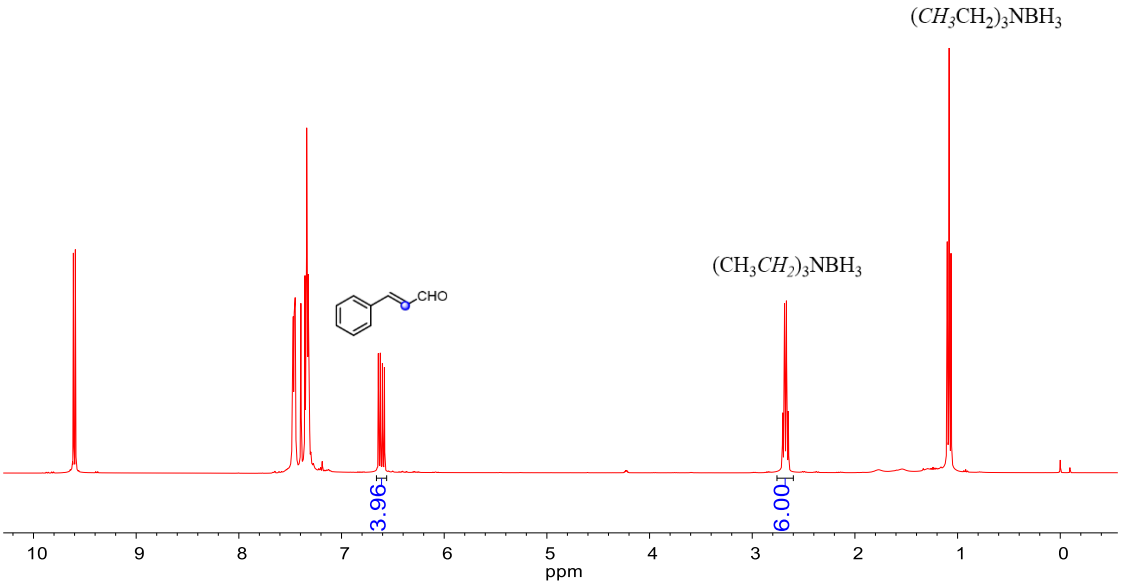

Figure S16. ^1H NMR spectra in $CDCl_3$ for the reaction of Et_3NBH_3 with cinnamaldehyde in THF for 3d at room temperature.

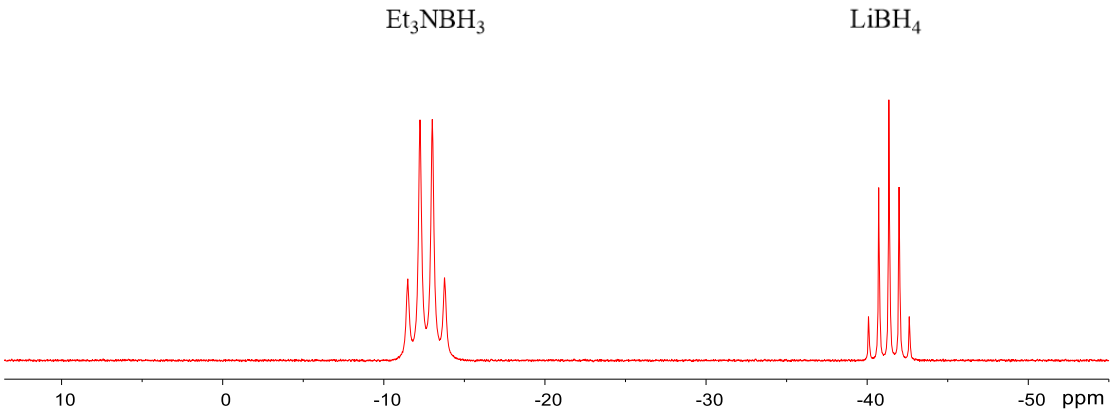

Figure S17. ^{11}B NMR spectra for the reaction of cinnamaldehyde, $LiBH_4$, and Et_3N at 2 : 1 : 4 ratio in THF.

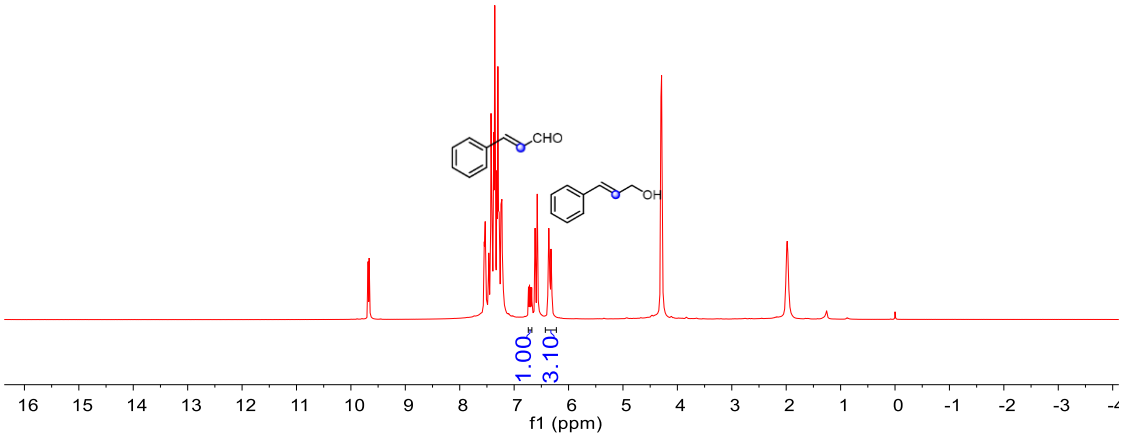

Figure S18. ^{1}H NMR spectra in $CDCl_3$ for the reaction of $LiBH_4$ with cinnamaldehyde in THF without Et_3N.

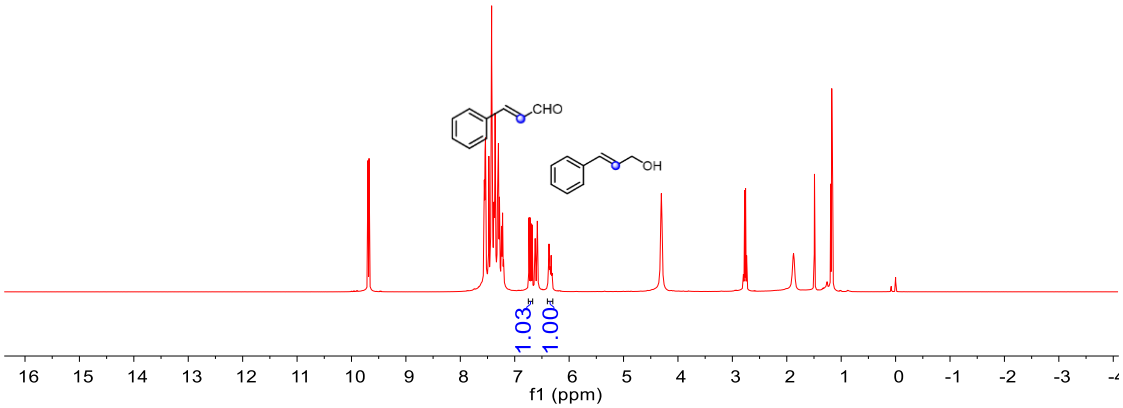

Figure S19. $^{1}H\{^{11}B\}$ NMR spectra in $CDCl_3$ for the reaction of $LiBH_4$ with cinnamaldehyde in THF with 1 equiv. Et_3N.

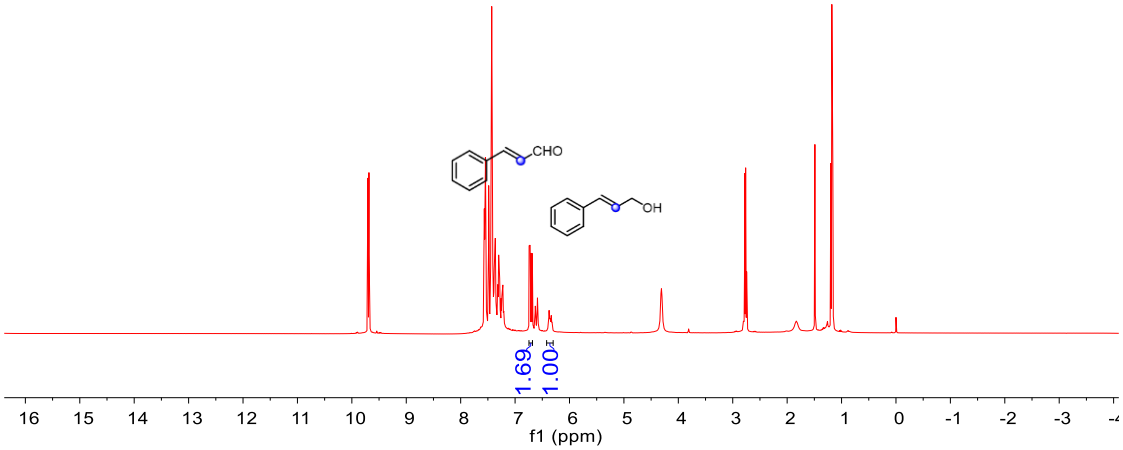

Figure S20. $^{1}H\{^{11}B\}$ NMR spectra in $CDCl_3$ for the reaction of $LiBH_4$ with cinnamaldehyde in THF with 2 equiv. Et_3N.

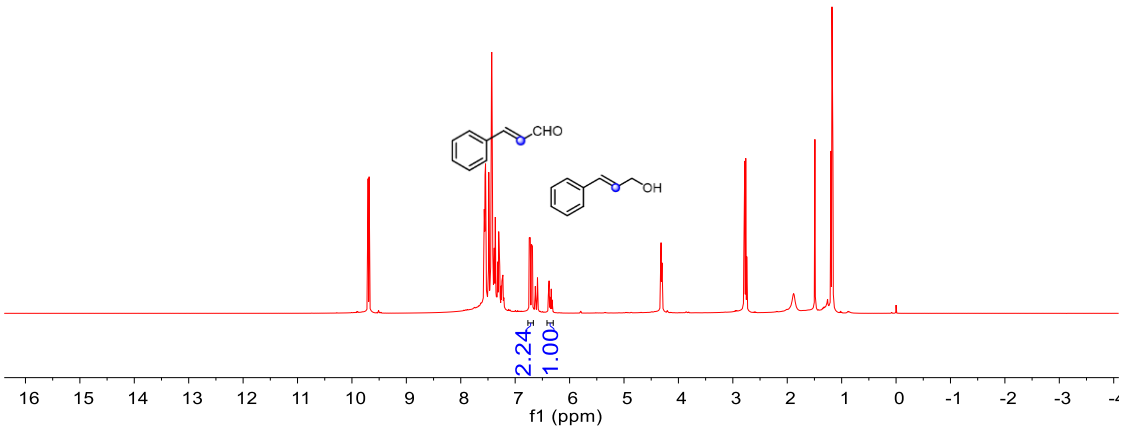

Figure S21. $^{1}H\{^{11}B\}$ NMR spectra in $CDCl_3$ for the reaction of $LiBH_4$ with cinnamaldehyde in THF with 3 equiv. Et_3N.

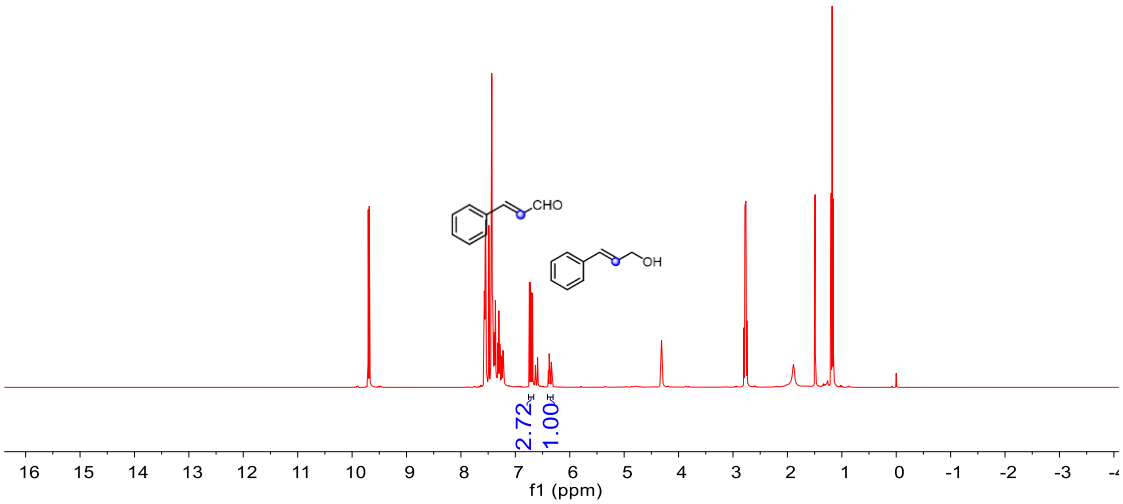

Figure S22. $^{1}H\{^{11}B\}$ NMR spectra in $CDCl_3$ for the reaction of $LiBH_4$ with cinnamaldehyde in THF with 4 equiv. Et_3N.

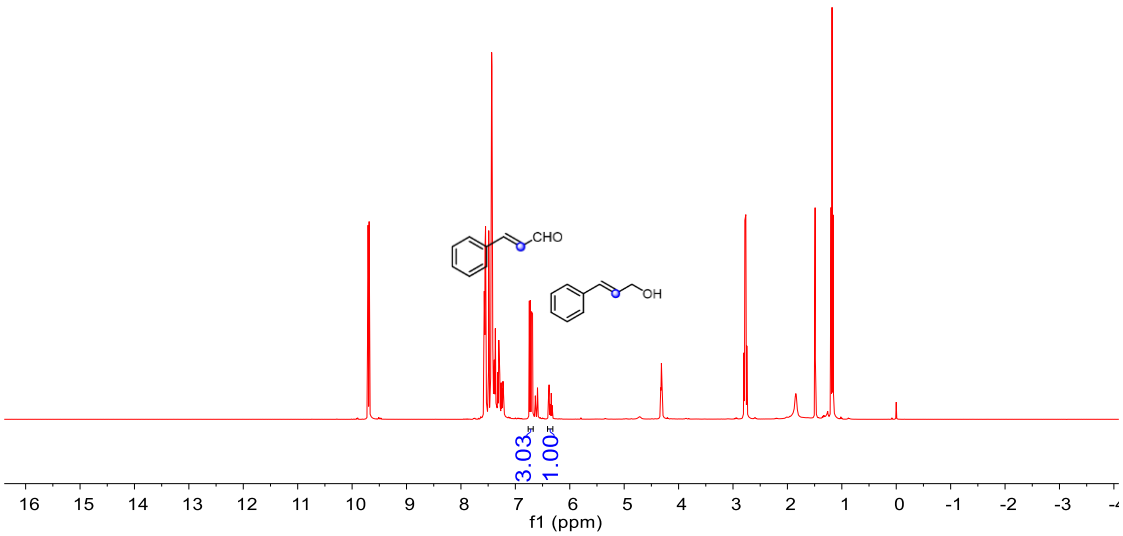

Figure S23. $^{1}H\{^{11}B\}$ NMR spectra in $CDCl_3$ for the reaction of $LiBH_4$ with cinnamaldehyde in THF with 5 equiv. Et_3N.

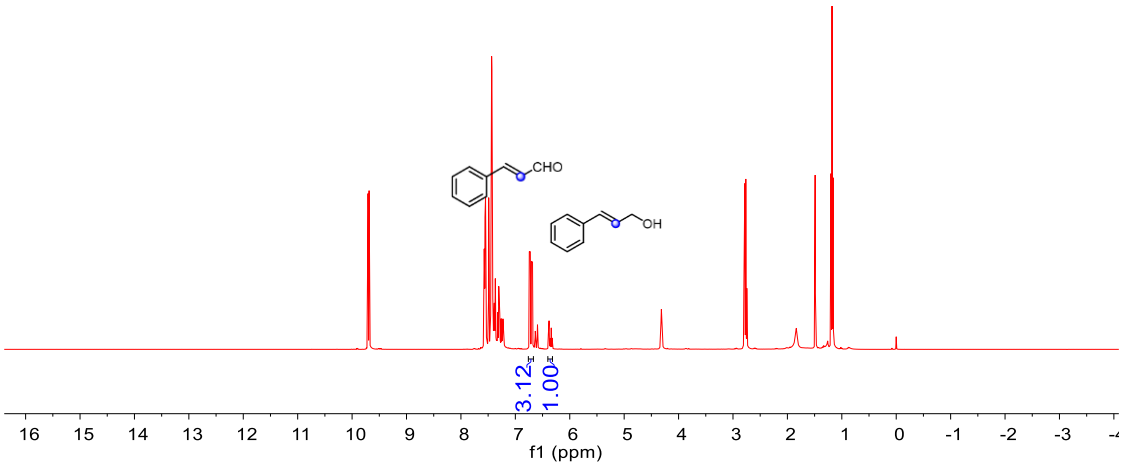

Figure S24. $^{1}H\{^{11}B\}$ NMR spectra in $CDCl_3$ for the reaction of $LiBH_4$ with cinnamaldehyde in THF with 7.5 equiv. Et_3N.

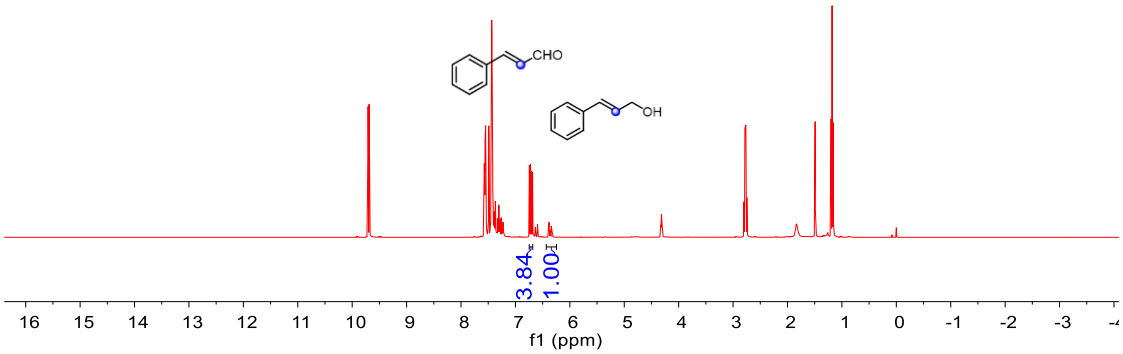

Figure S25. $^{1}H\{^{11}B\}$ NMR spectra in $CDCl_3$ for the reaction of $LiBH_4$ with cinnamaldehyde in THF with 10 equiv. Et_3N.

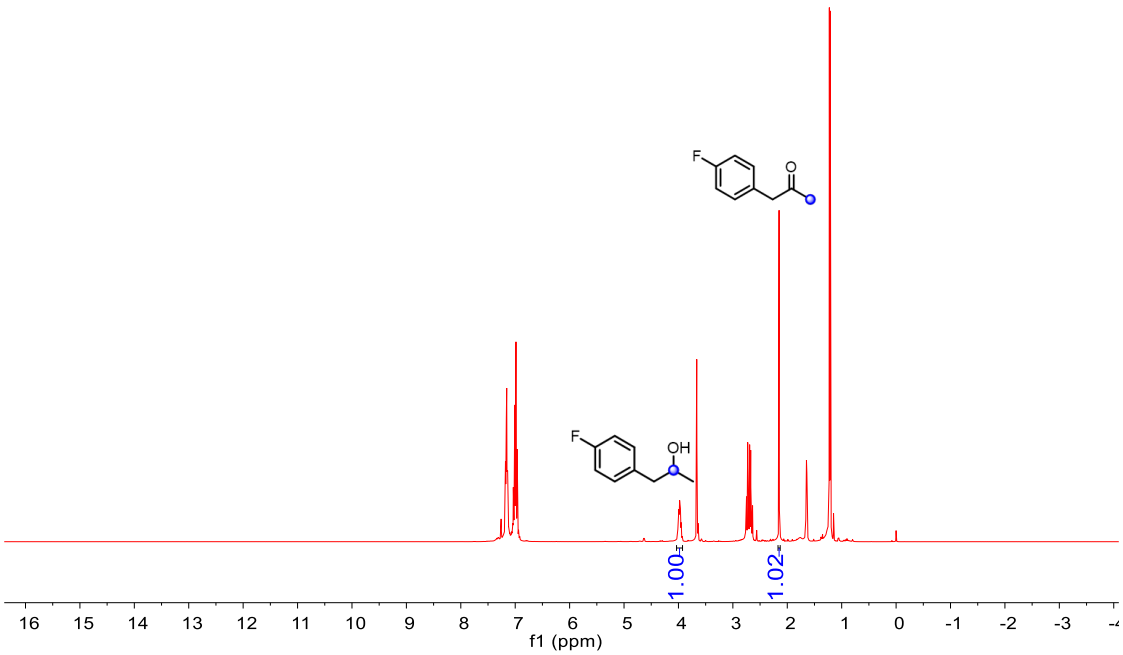

Figure S26. ^{1}H NMR spectra in $CDCl_3$ for the reaction of $LiBH_4$ with 4-fluorophenylacetone in THF without Et_3N.

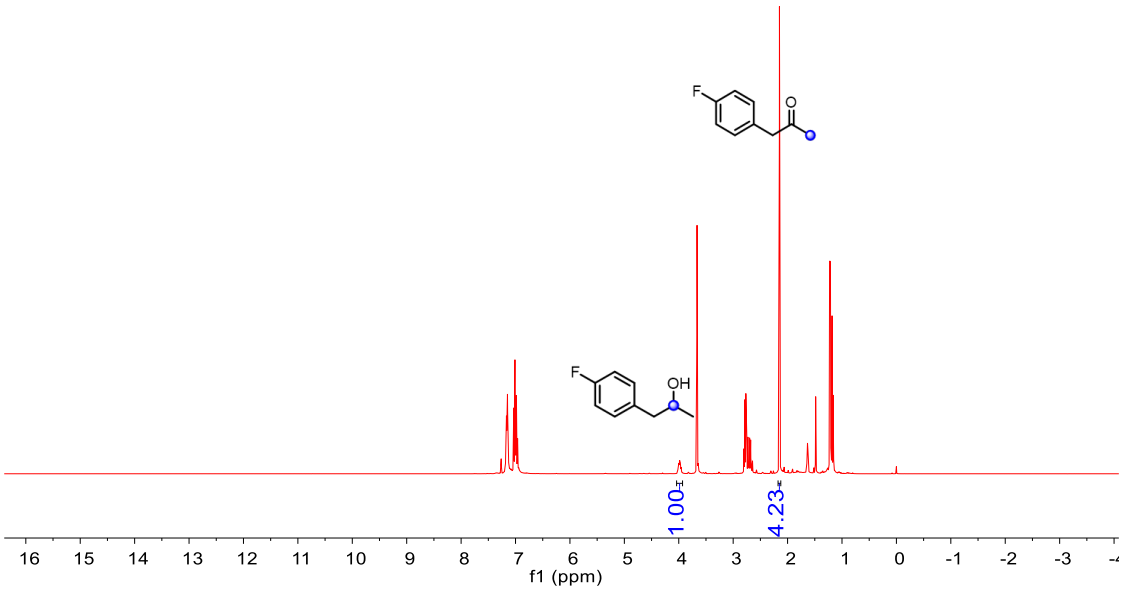

Figure S27. $^{1}H\{^{11}B\}$ NMR spectra in $CDCl_3$ for the reaction of $LiBH_4$ with 4-fluorophenylacetone in THF with 1 equiv. Et_3N.

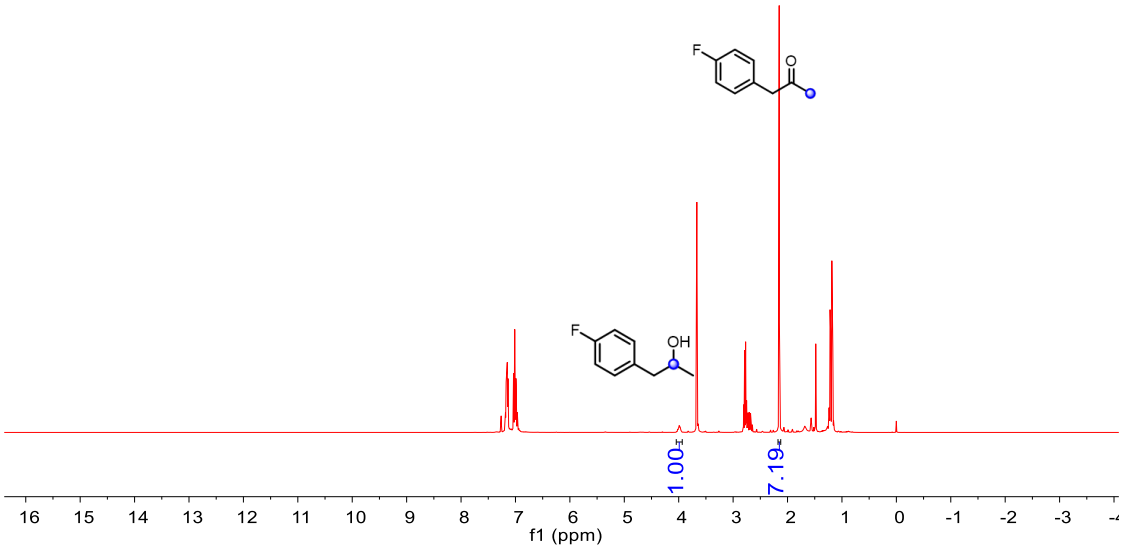

Figure S28. $^{1}H\{^{11}B\}$ NMR spectra in $CDCl_3$ for the reaction of $LiBH_4$ with 4-fluorophenylacetone in THF with 2 equiv. Et_3N.

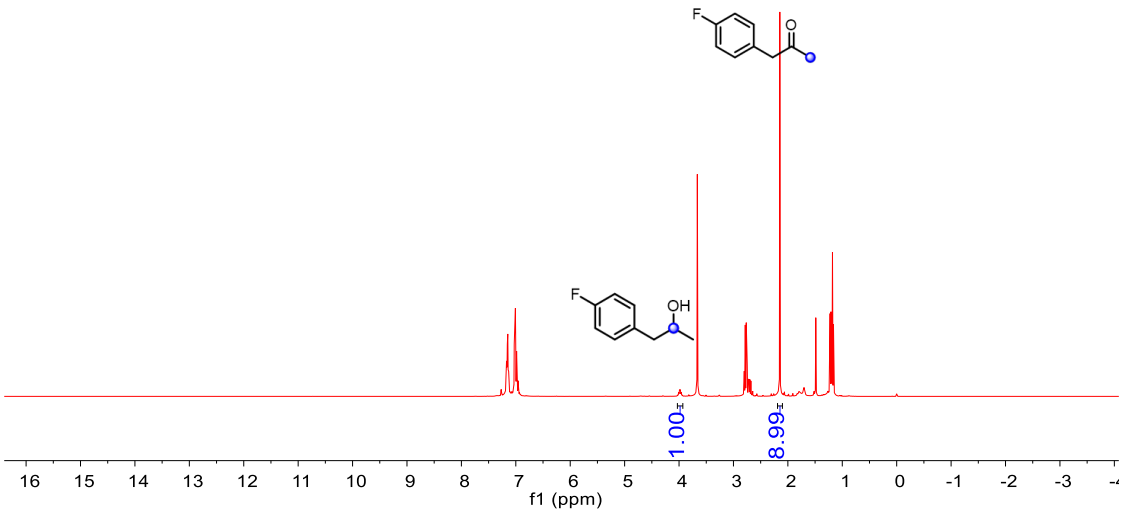

Figure S29. $^{1}H\{^{11}B\}$ NMR spectra in $CDCl_3$ for the reaction of $LiBH_4$ with 4-fluorophenylacetone in THF with 3 equiv. Et_3N.

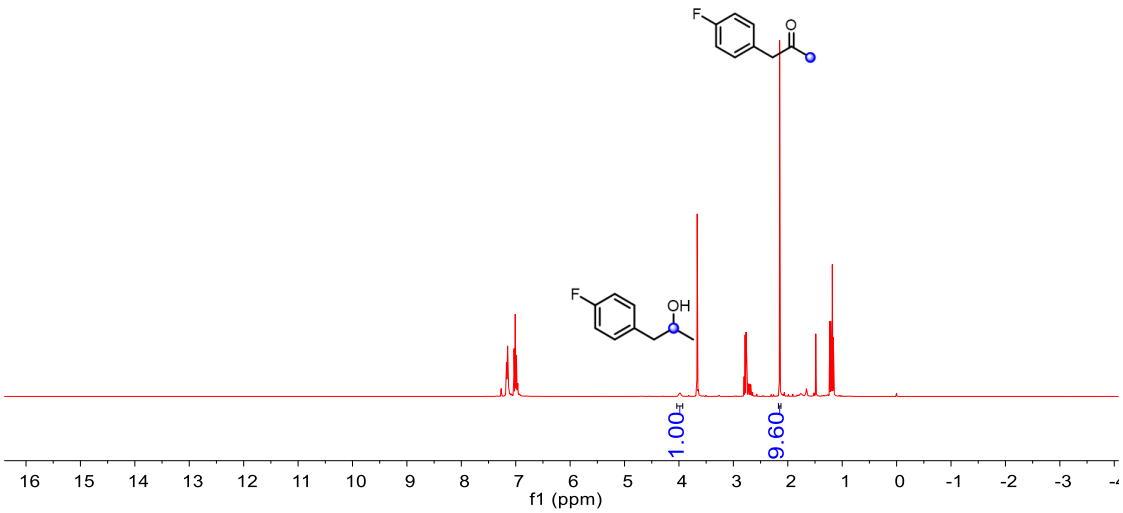

Figure S30. $^{1}H\{^{11}B\}$ NMR spectra in $CDCl_3$ for the reaction of $LiBH_4$ with 4-fluorophenylacetone in THF with 4 equiv. Et_3N.

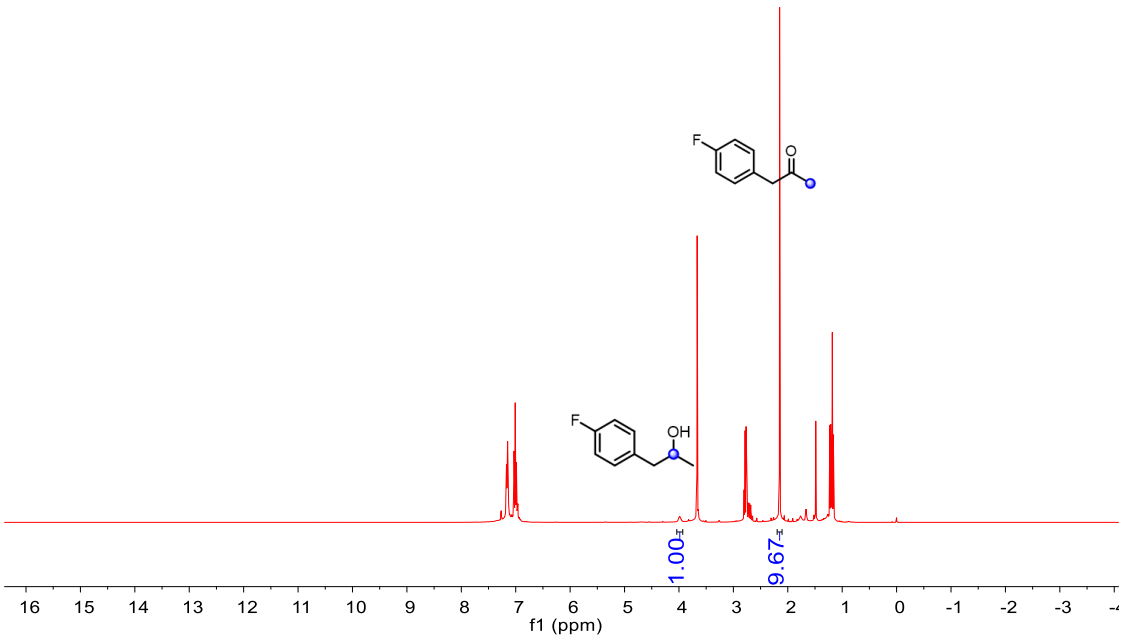

Figure S31. $^{1}H\{^{11}B\}$ NMR spectra in $CDCl_3$ for the reaction of $LiBH_4$ with 4-fluorophenylacetone in THF with 5 equiv. Et_3N.

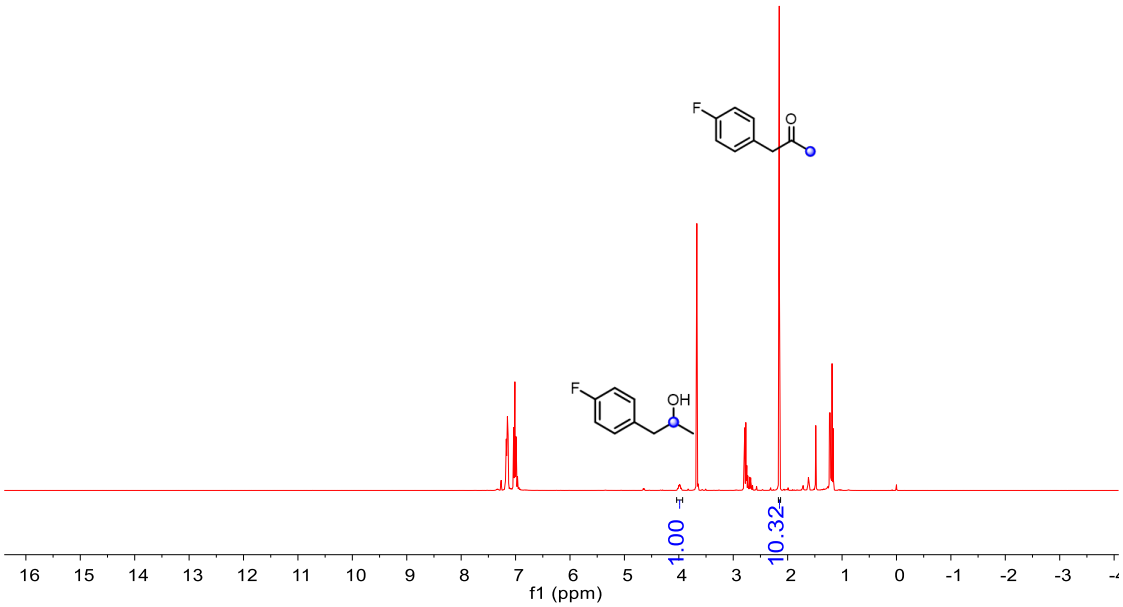

Figure S32. $^{1}H\{^{11}B\}$ NMR spectra in $CDCl_3$ for the reaction of $LiBH_4$ with 4-fluorophenylacetone in THF with 7.5 equiv. Et_3N.

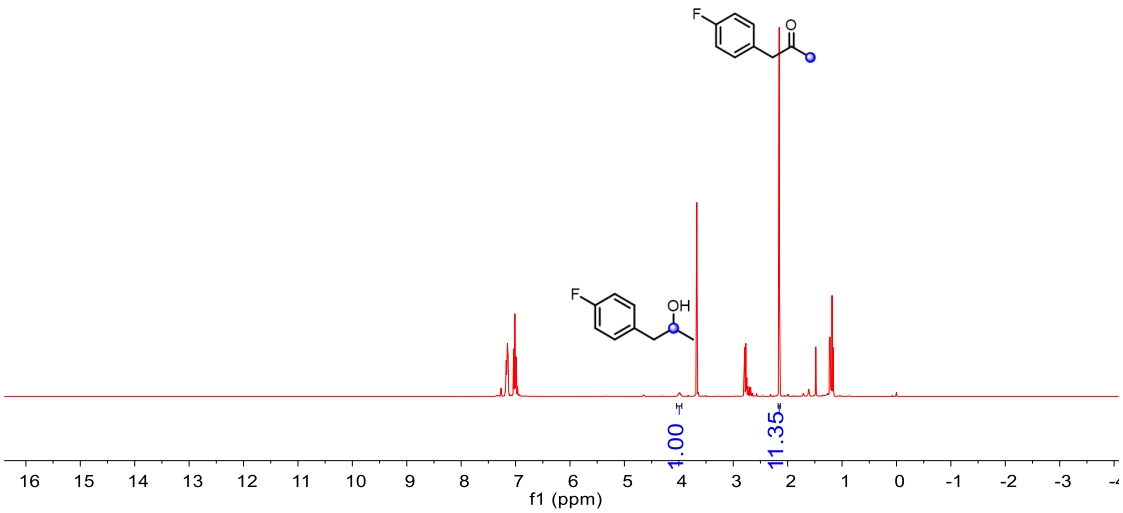

Figure S33. $^{1}H\{^{11}B\}$ NMR spectra in $CDCl_3$ for the reaction of $LiBH_4$ with 4-fluorophenylacetone in THF with 10 equiv. Et_3N.

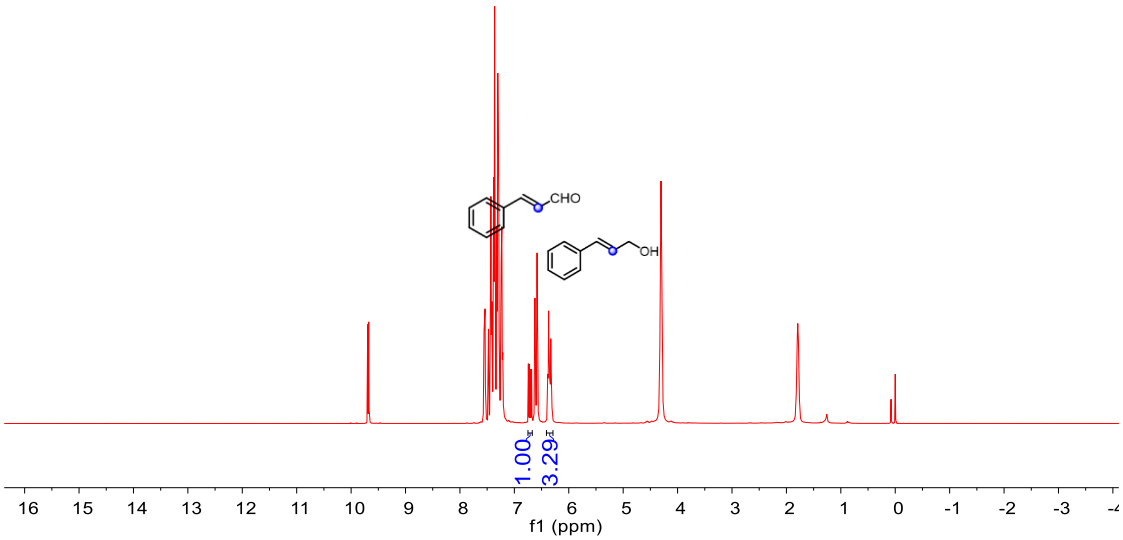

Figure S34. ^{1}H NMR spectra in $CDCl_3$ for the reaction of $Ca(BH_4)_2$ with cinnamaldehyde in THF without Et_3N.

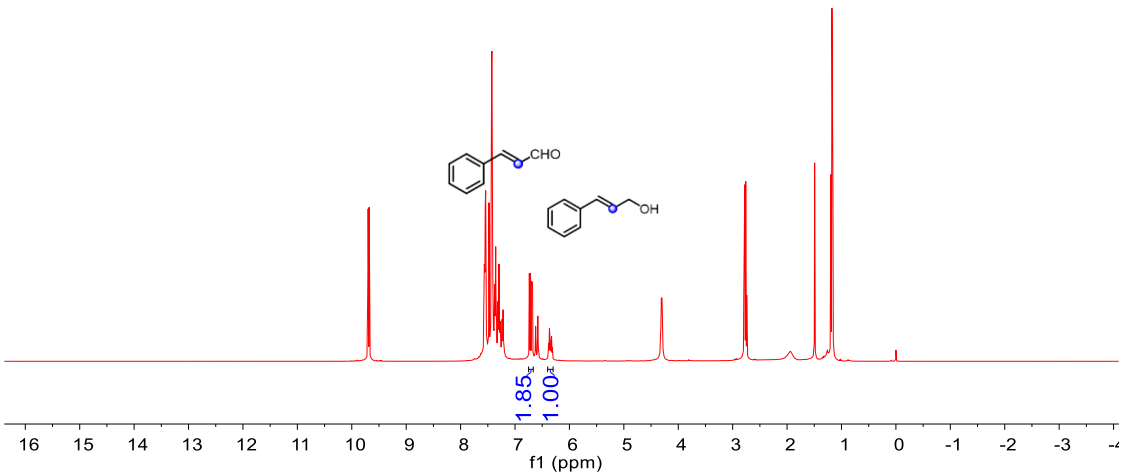

Figure S35. $^{1}H\{^{11}B\}$ NMR spectra in $CDCl_3$ for the reaction of $Ca(BH_4)_2$ with cinnamaldehyde in THF with 1 equiv. Et_3N.

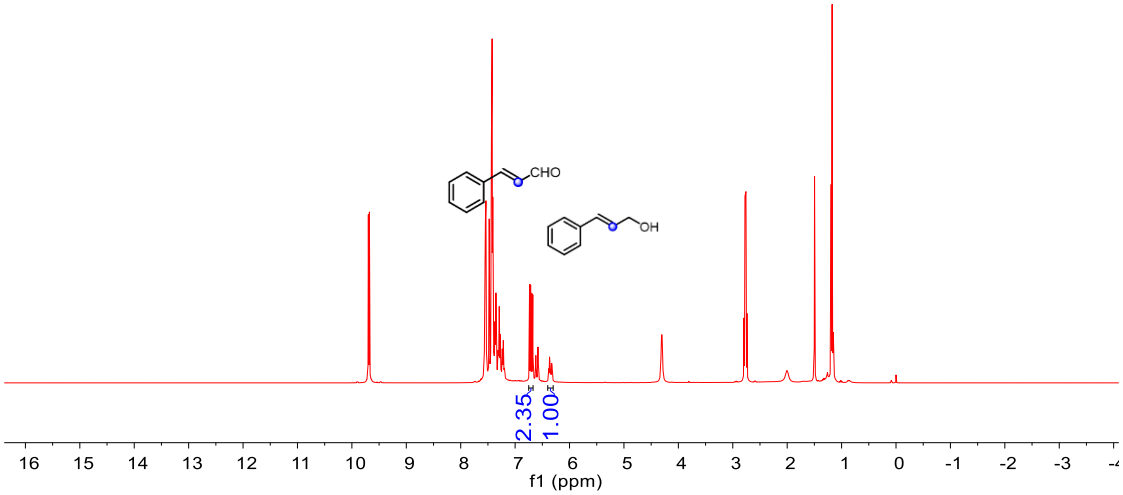

Figure S36. $^{1}H\{^{11}B\}$ NMR spectra in $CDCl_3$ for the reaction of $Ca(BH_4)_2$ with cinnamaldehyde in THF with 2 equiv. Et_3N.

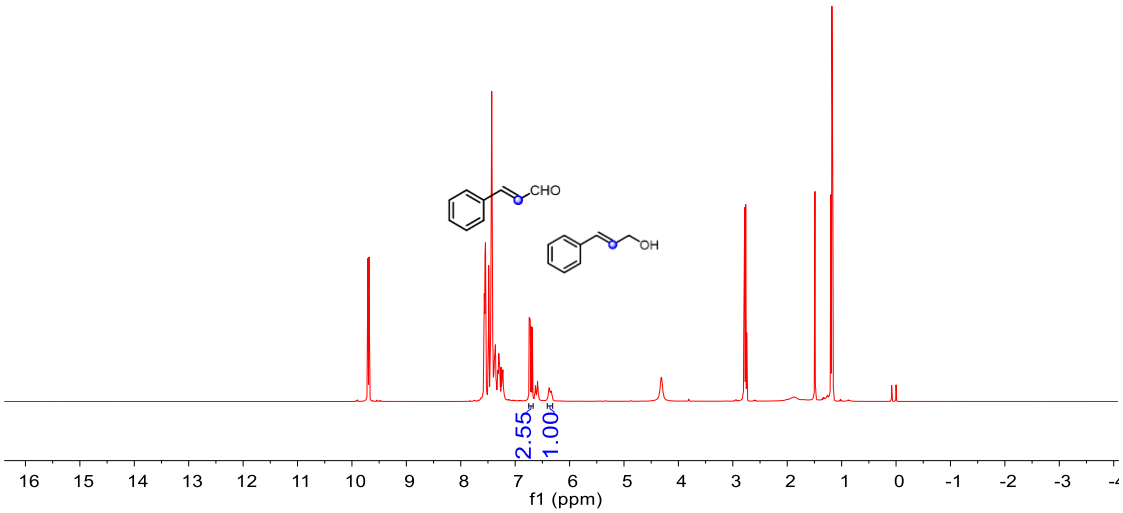

Figure S37. $^{1}H\{^{11}B\}$ NMR spectra in $CDCl_3$ for the reaction of $Ca(BH_4)_2$ with cinnamaldehyde in THF with 3 equiv. Et_3N.

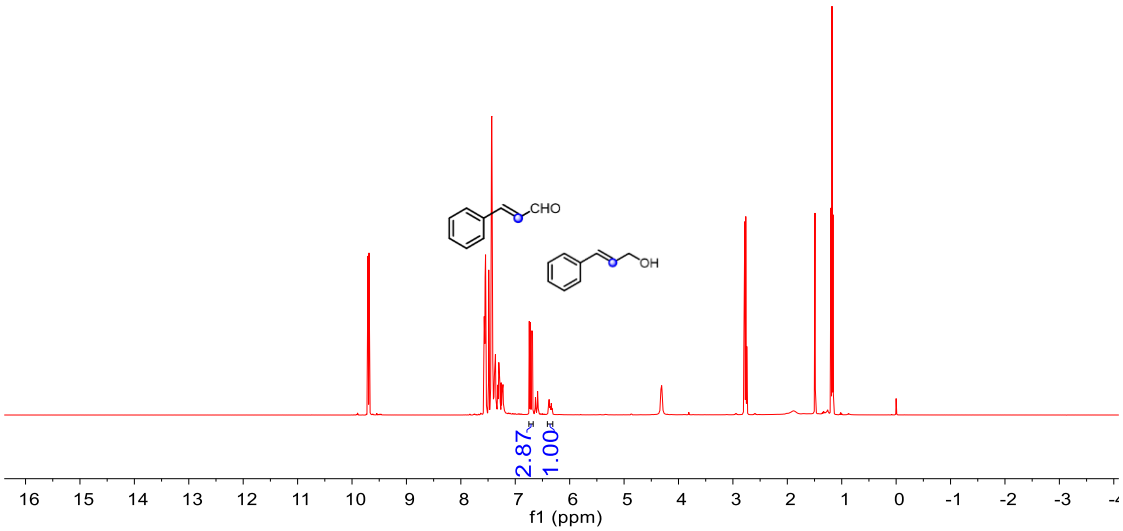

Figure S38. $^{1}H\{^{11}B\}$ NMR spectra in $CDCl_3$ for the reaction of $Ca(BH_4)_2$ with cinnamaldehyde in THF with 4 equiv. Et_3N.

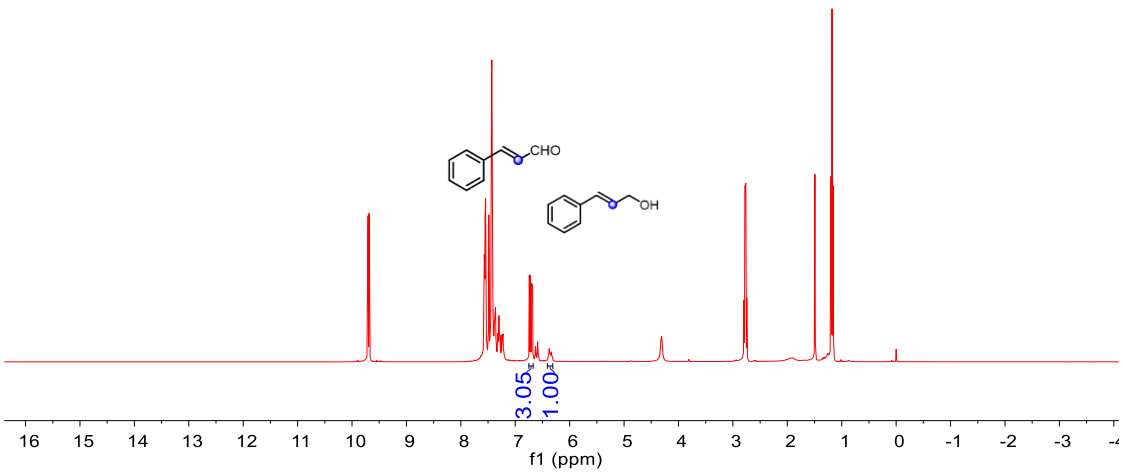

Figure S39. $^{1}H\{^{11}B\}$ NMR spectra in $CDCl_3$ for the reaction of $Ca(BH_4)_2$ with cinnamaldehyde in THF with 5 equiv. Et_3N.

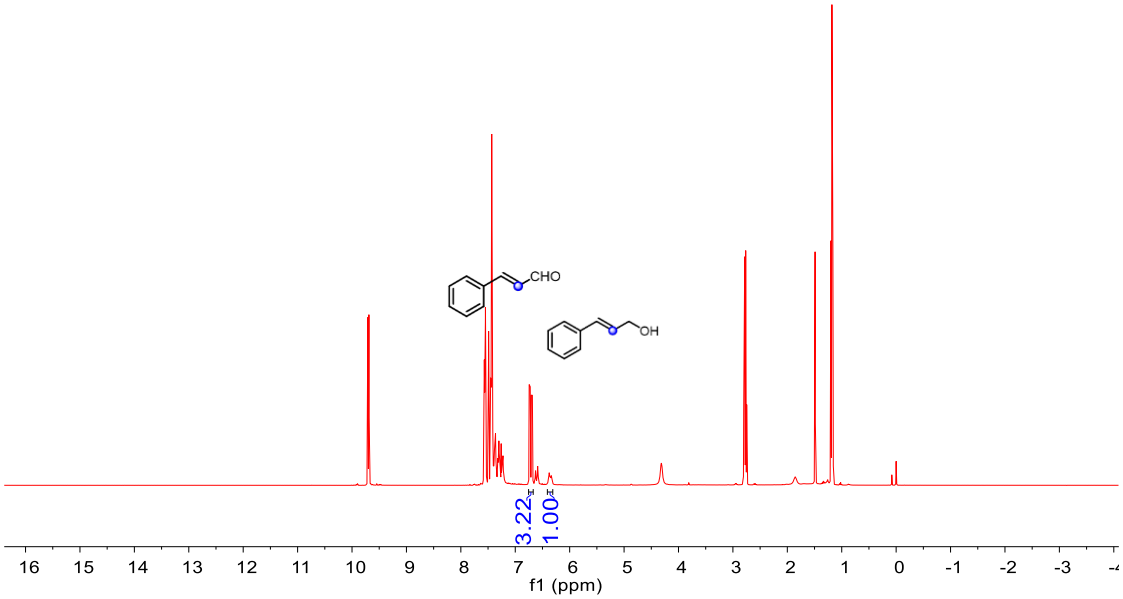

Figure S40. $^{1}H\{^{11}B\}$ NMR spectra in $CDCl_3$ for the reaction of $Ca(BH_4)_2$ with cinnamaldehyde in THF with 7.5 equiv. Et_3N.

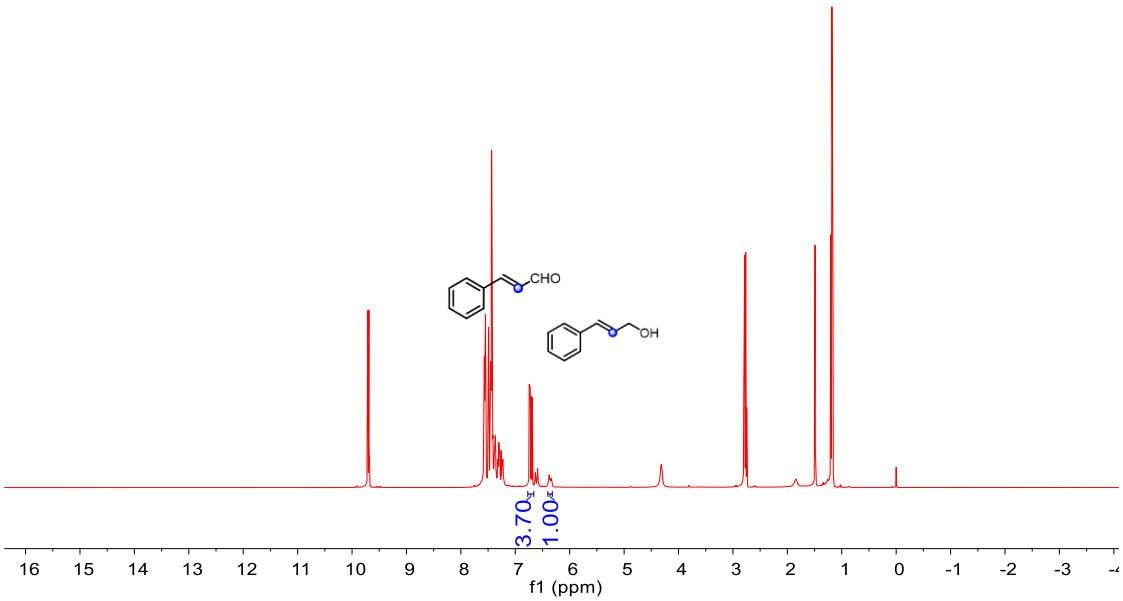

Figure S41. $^{1}H\{^{11}B\}$ NMR spectra in $CDCl_3$ for the reaction of $Ca(BH_4)_2$ with cinnamaldehyde in THF with 10 equiv. Et_3N.

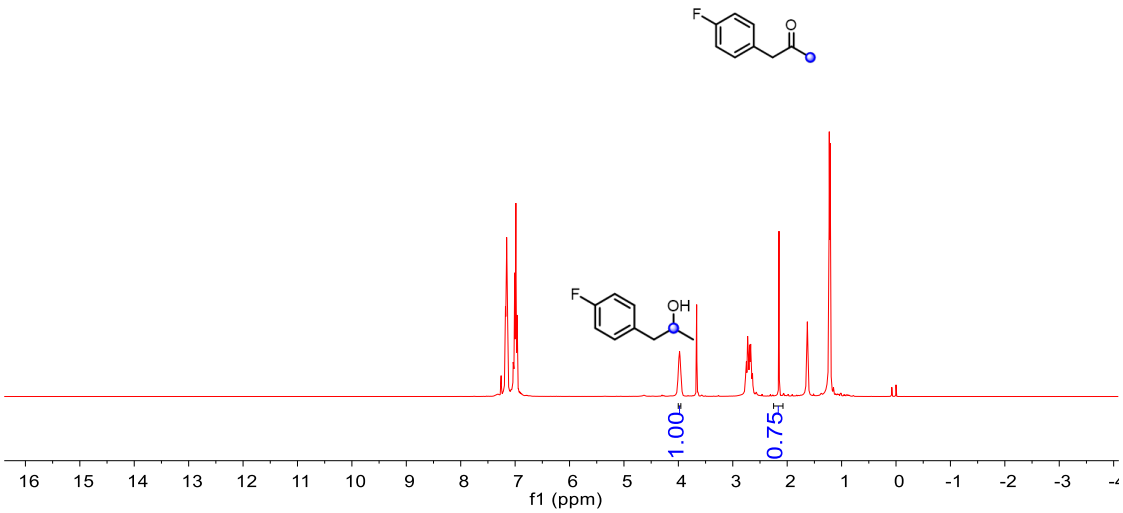

Figure S42. ^{1}H NMR spectra in $CDCl_3$ for the reaction of $Ca(BH_4)_2$ with 4-fluorophenylacetone in THF without Et_3N.

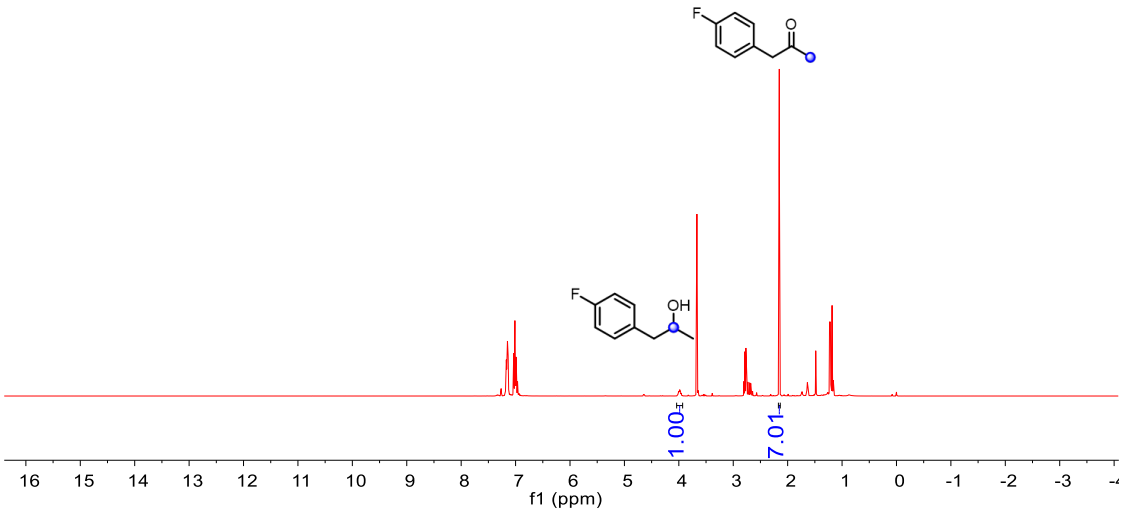

Figure S43. $^{1}H\{^{11}B\}$ NMR spectra in $CDCl_3$ for the reaction of $Ca(BH_4)_2$ with 4-fluorophenylacetone in THF with 1 equiv. Et_3N.

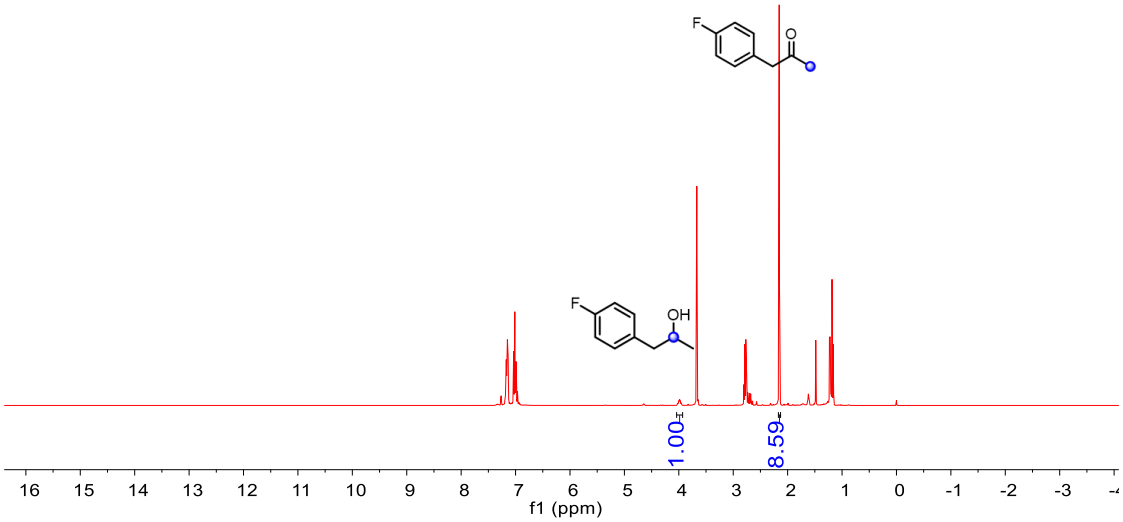

Figure S44. $^{1}H\{^{11}B\}$ NMR spectra in $CDCl_3$ for the reaction of $Ca(BH_4)_2$ with 4-fluorophenylacetone in THF with 2 equiv. Et_3N.

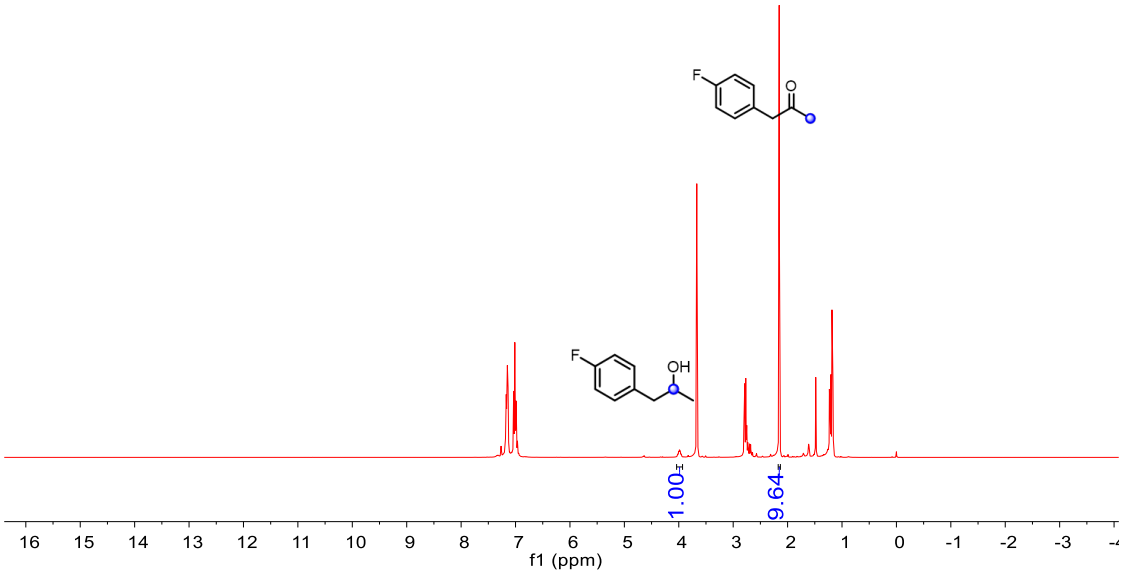

Figure S45. $^{1}H\{^{11}B\}$ NMR spectra in $CDCl_3$ for the reaction of $Ca(BH_4)_2$ with 4-fluorophenylacetone in THF with 3 equiv. Et_3N.

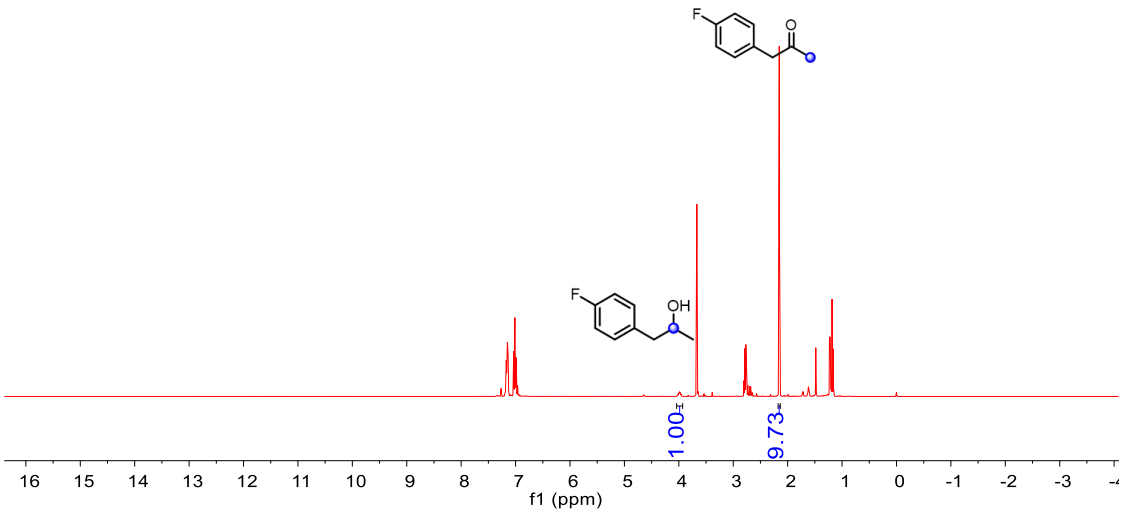

Figure S46. $^{1}H\{^{11}B\}$ NMR spectra in $CDCl_3$ for the reaction of $Ca(BH_4)_2$ with 4-fluorophenylacetone in THF with 4 equiv. Et_3N.

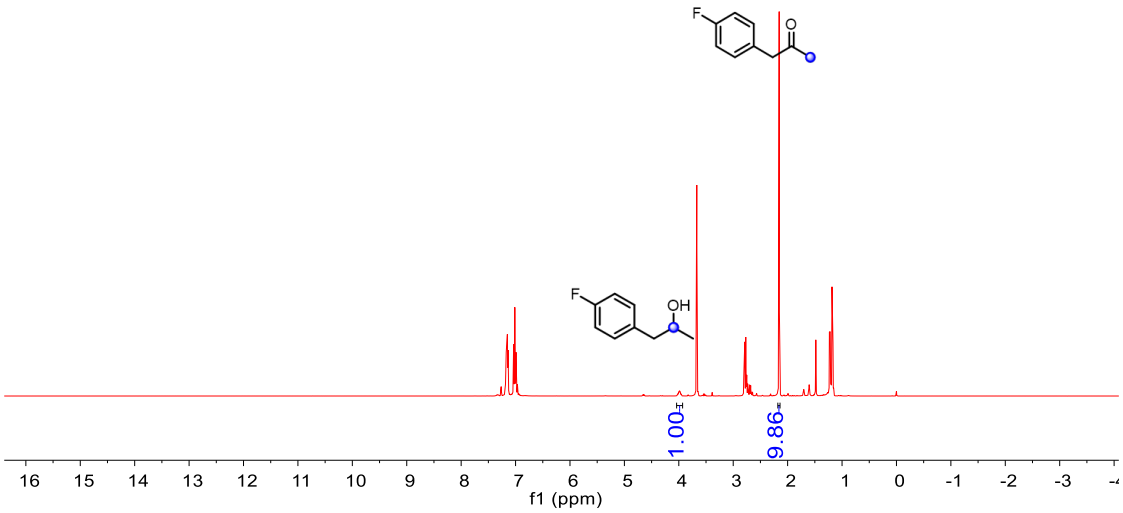

Figure S47. $^{1}H\{^{11}B\}$ NMR spectra in $CDCl_3$ for the reaction of $Ca(BH_4)_2$ with 4-fluorophenylacetone in THF with 5 equiv. Et_3N.

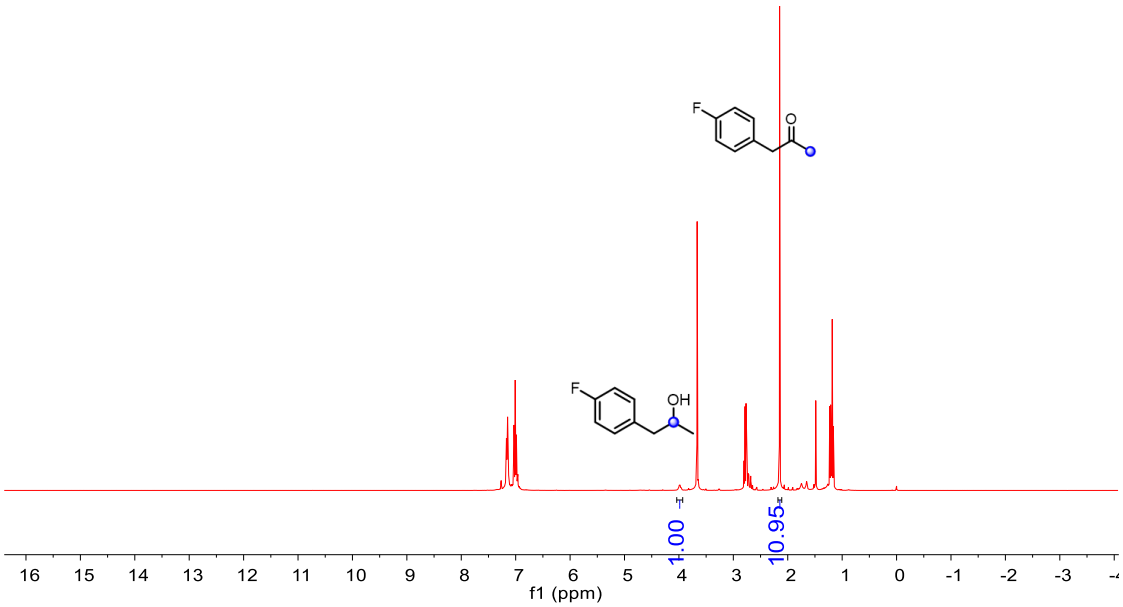

Figure S48. $^{1}H\{^{11}B\}$ NMR spectra in $CDCl_3$ for the reaction of $Ca(BH_4)_2$ with 4-fluorophenylacetone in THF with 7.5 equiv. Et_3N.

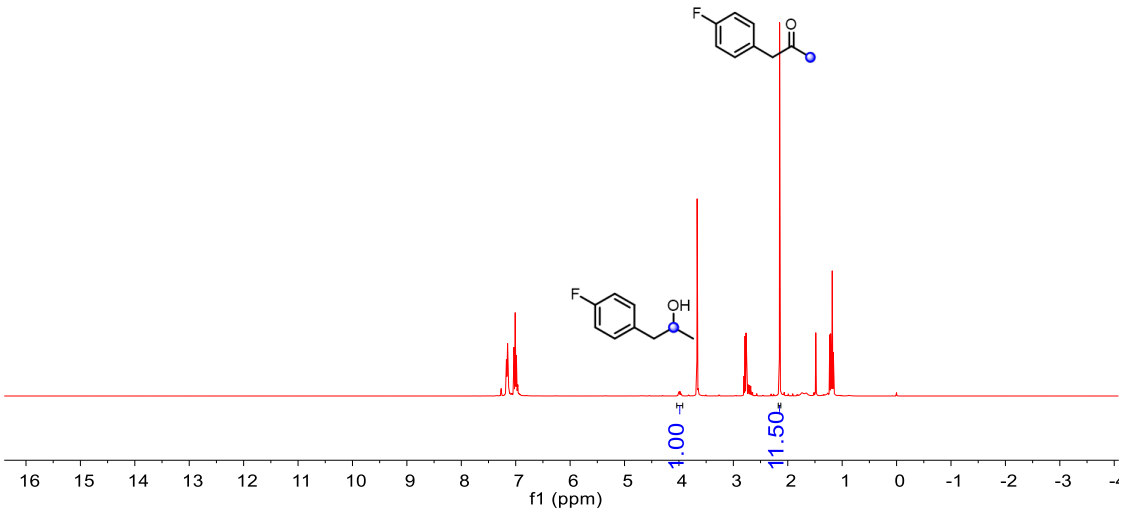

Figure S49. $^{1}H\{^{11}B\}$ NMR spectra in $CDCl_3$ for the reaction of $Ca(BH_4)_2$ with 4-fluorophenylacetone in THF with 10 equiv. Et_3N.

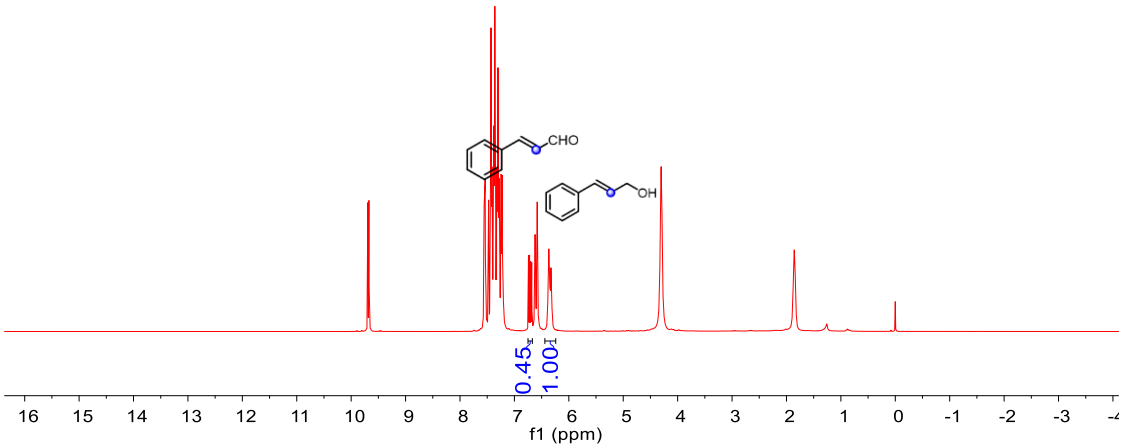

Figure S50. ^{1}H NMR spectra in $CDCl_3$ for the reaction of $LiBH_4$ with cinnamaldehyde in DME without Et_3N.

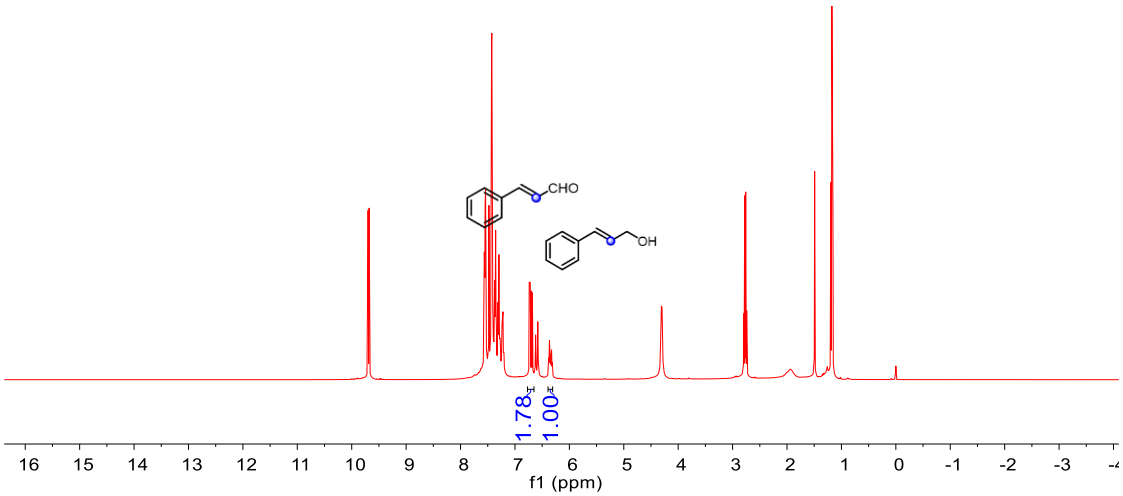

Figure S51. $^{1}H\{^{11}B\}$ NMR spectra in $CDCl_3$ for the reaction of $LiBH_4$ with cinnamaldehyde in DME with 1 equiv. Et_3N.

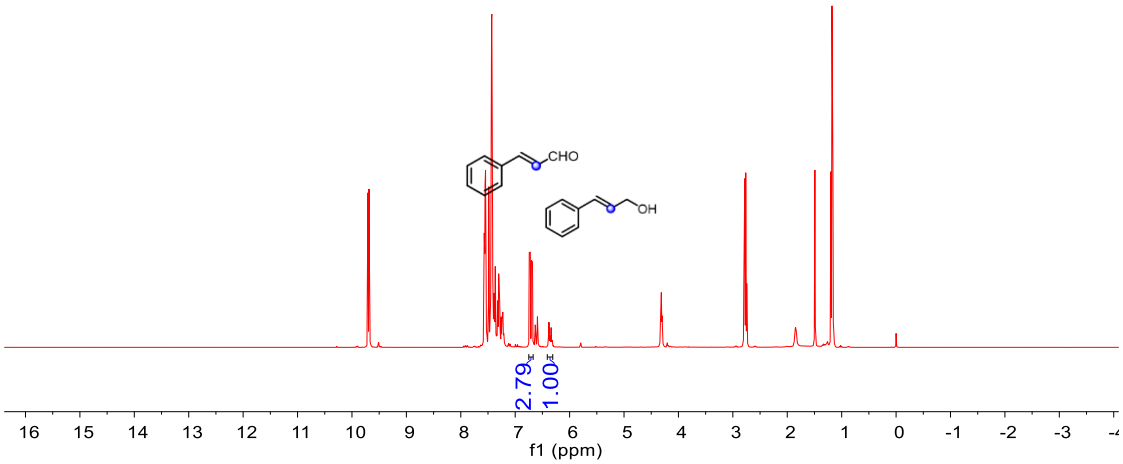

Figure S52. $^{1}H\{^{11}B\}$ NMR spectra in $CDCl_3$ for the reaction of $LiBH_4$ with cinnamaldehyde in DME with 2 equiv. Et_3N.

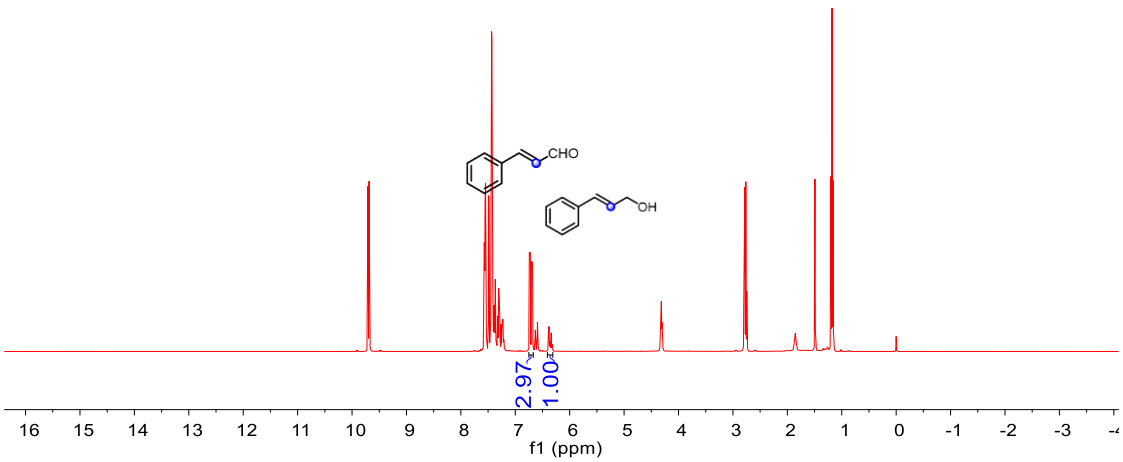

Figure S53. $^{1}H\{^{11}B\}$ NMR spectra in $CDCl_3$ for the reaction of $LiBH_4$ with cinnamaldehyde in DME with 3 equiv. Et_3N.

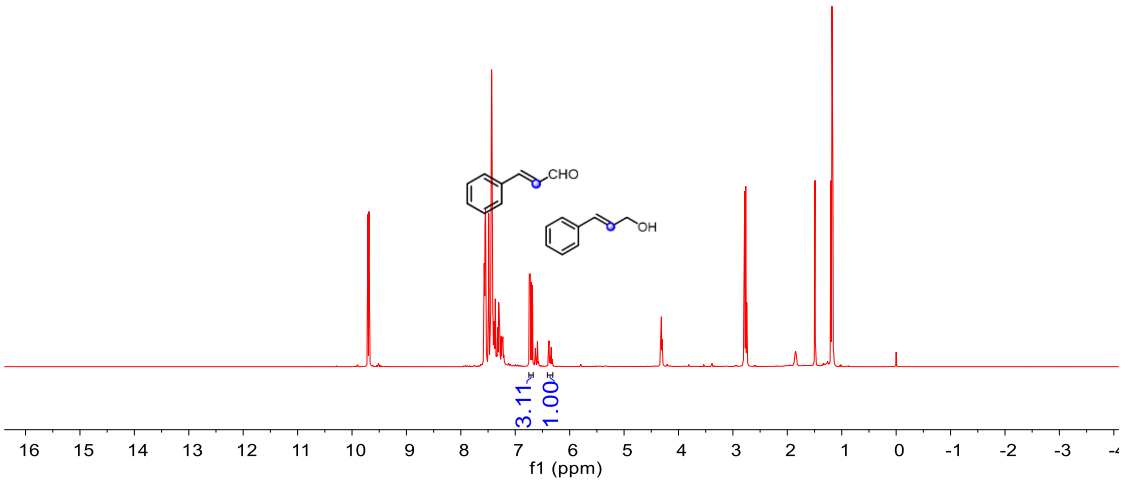

Figure S54. $^{1}H\{^{11}B\}$ NMR spectra in $CDCl_3$ for the reaction of $LiBH_4$ with cinnamaldehyde in DME with 4 equiv. Et_3N.

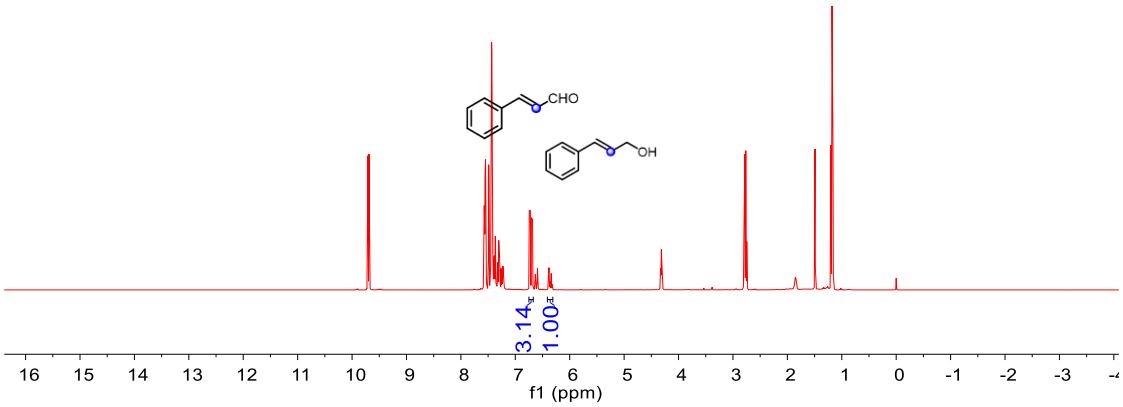

Figure S55. $^{1}H\{^{11}B\}$ NMR spectra in $CDCl_3$ for the reaction of $LiBH_4$ with cinnamaldehyde in DME with 5 equiv. Et_3N.

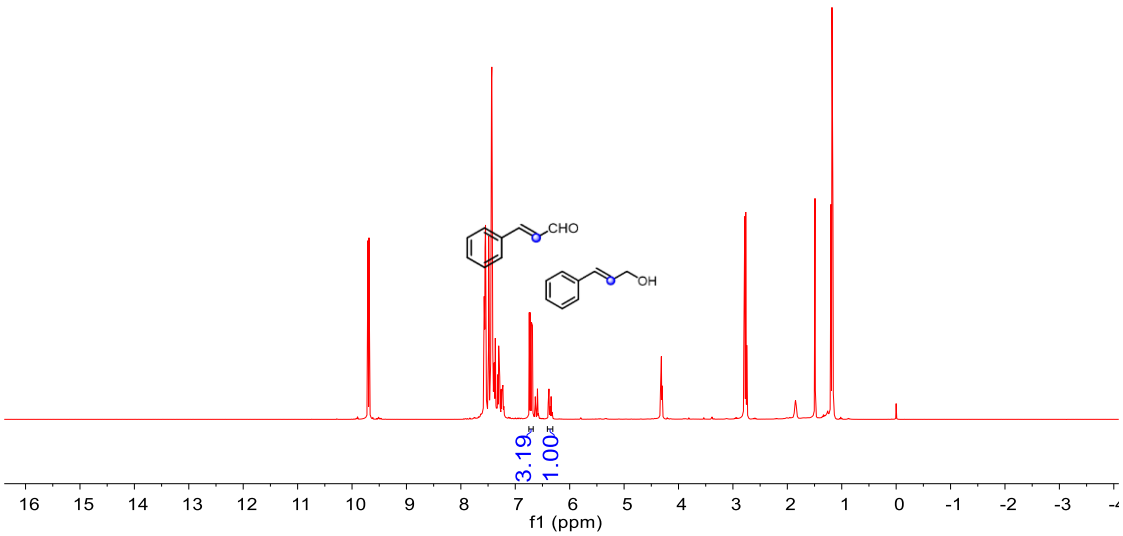

Figure S56. $^{1}H\{^{11}B\}$ NMR spectra in $CDCl_3$ for the reaction of $LiBH_4$ with cinnamaldehyde in DME with 7.5 equiv. Et_3N.

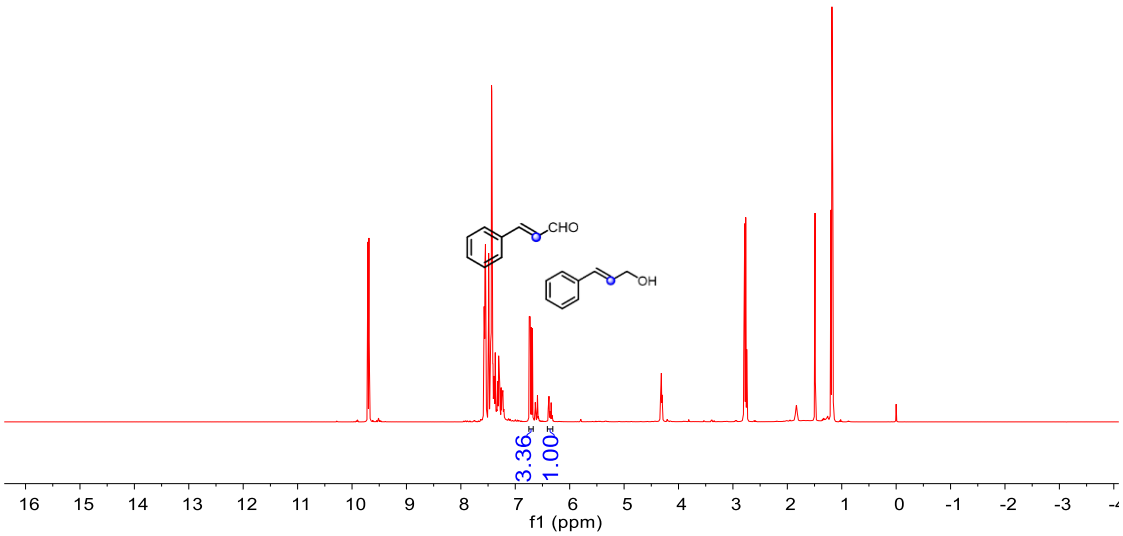

Figure S57. $^{1}H\{^{11}B\}$ NMR spectra in $CDCl_3$ for the reaction of $LiBH_4$ with cinnamaldehyde in DME with 10 equiv. Et_3N.

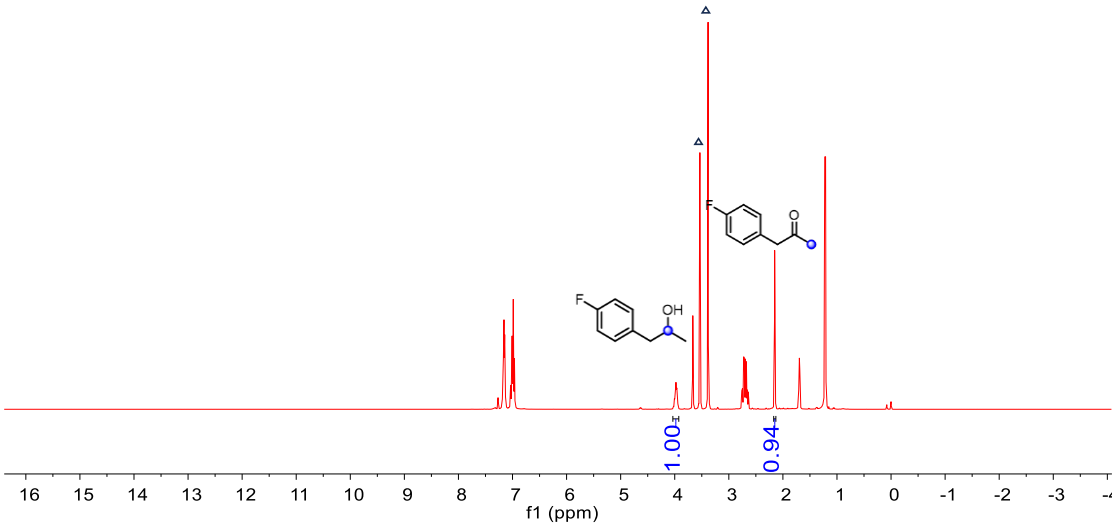

Figure S58. ^{1}H NMR spectra in $CDCl_3$ for the reaction of $LiBH_4$ with 4-fluorophenylacetone in DME without Et_3N (△stands for solvent, DME).

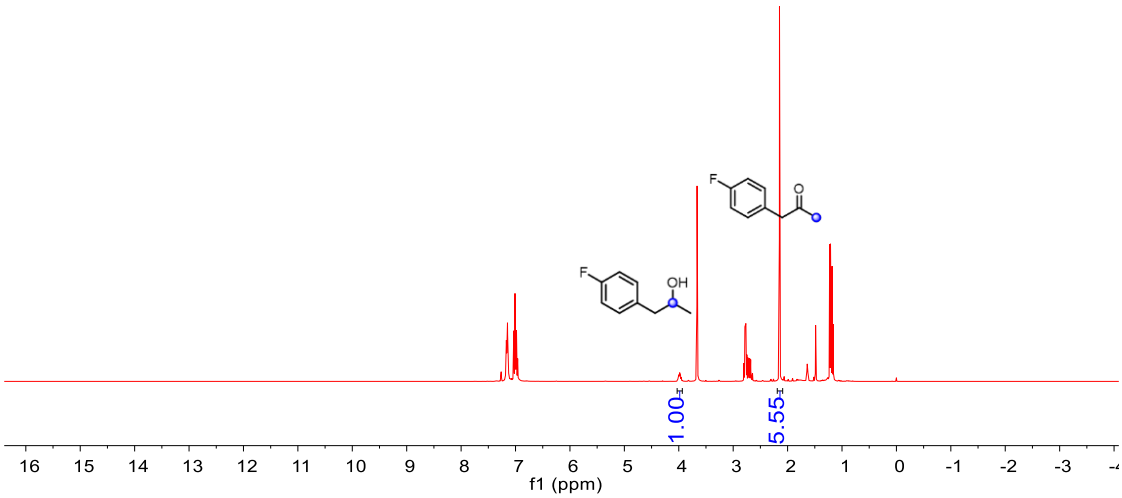

Figure S59. $^{1}H\{^{11}B\}$ NMR spectra in $CDCl_3$ for the reaction of $LiBH_4$ with 4-fluorophenylacetone in DME with 1 equiv. Et_3N.

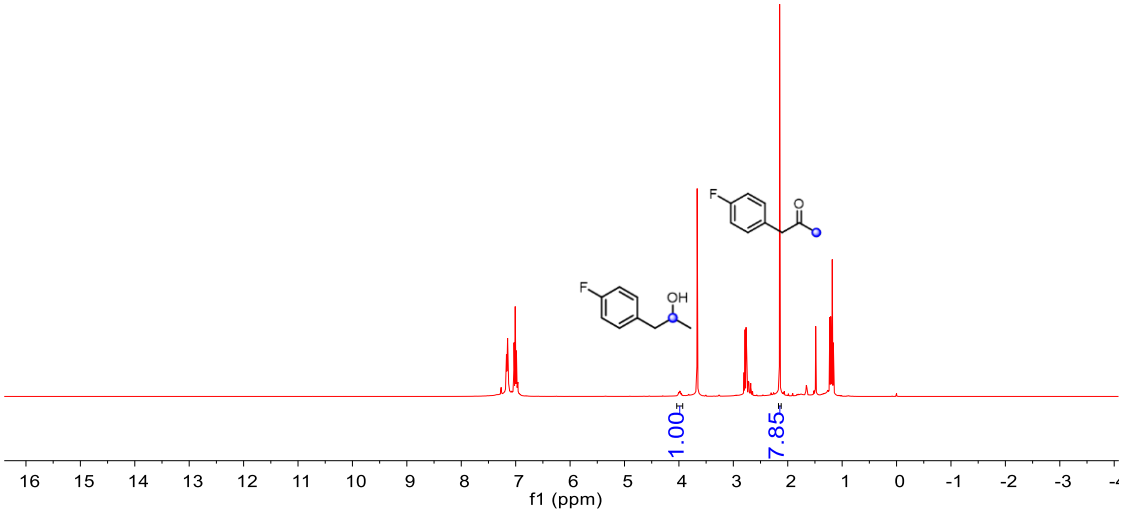

Figure S60. $^{1}H\{^{11}B\}$ NMR spectra in $CDCl_3$ for the reaction of $LiBH_4$ with 4-fluorophenylacetone in DME with 2 equiv. Et_3N.

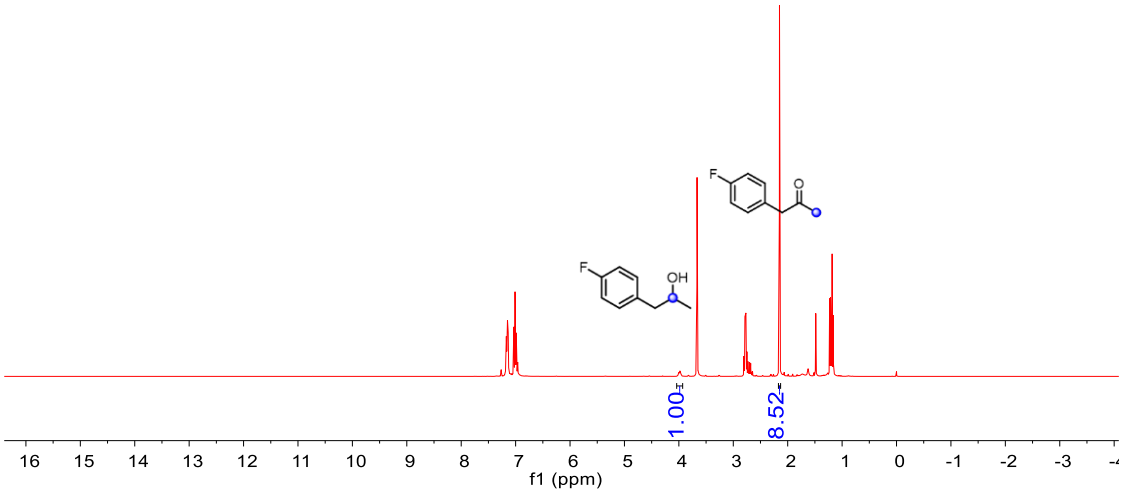

Figure S61. $^{1}H\{^{11}B\}$ NMR spectra in $CDCl_3$ for the reaction of $LiBH_4$ with 4-fluorophenylacetone in DME with 3 equiv. Et_3N.

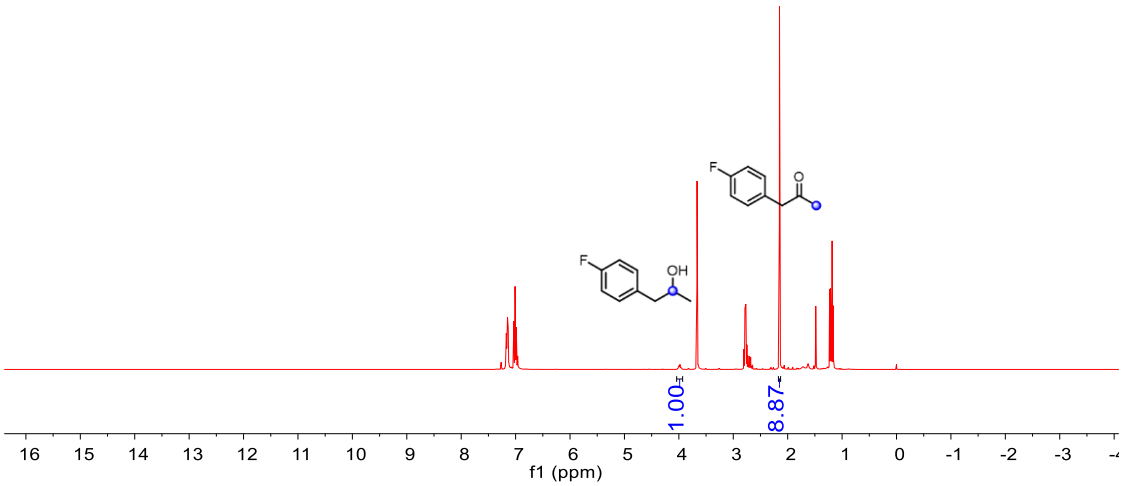

Figure S62. $^{1}H\{^{11}B\}$ NMR spectra in $CDCl_3$ for the reaction of $LiBH_4$ with 4-fluorophenylacetone in DME with 4 equiv. Et_3N.

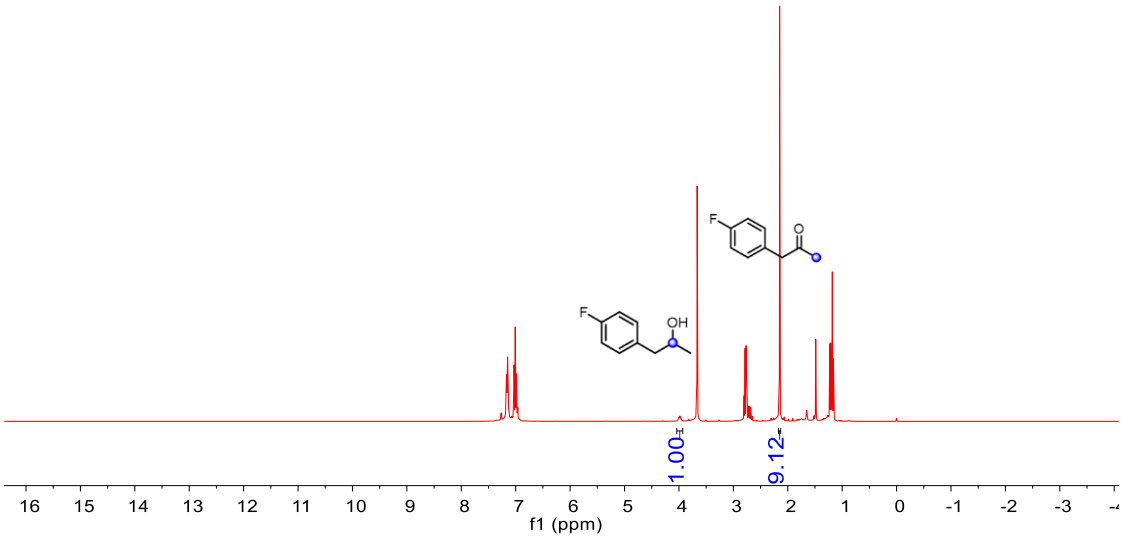

Figure S63. $^{1}H\{^{11}B\}$ NMR spectra in $CDCl_3$ for the reaction of $LiBH_4$ with 4-fluorophenylacetone in DME with 5 equiv. Et_3N.

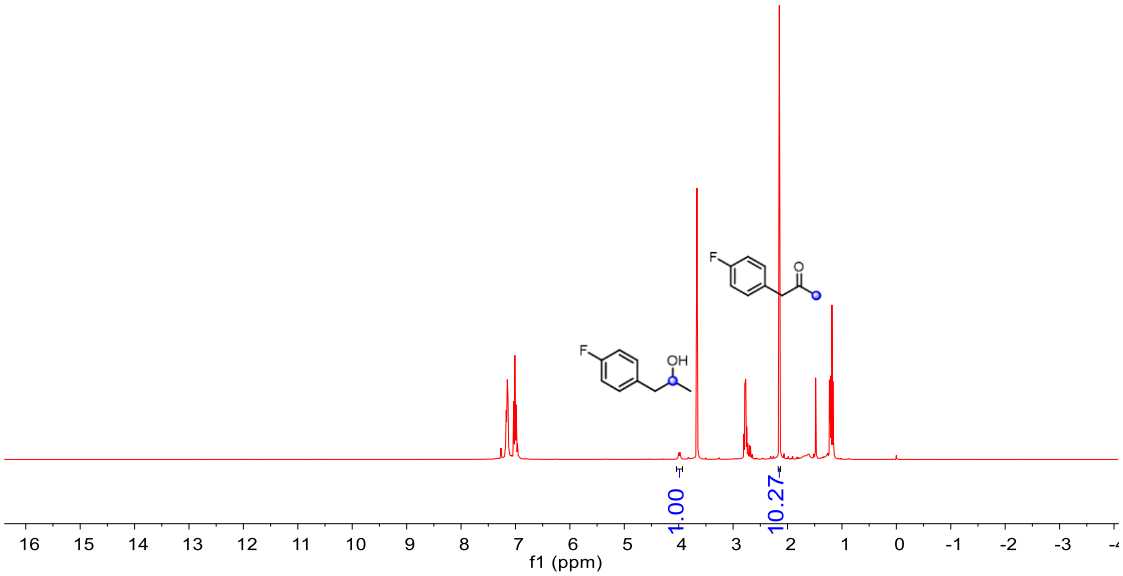

Figure S64. $^{1}H\{^{11}B\}$ NMR spectra in $CDCl_3$ for the reaction of $LiBH_4$ with 4-fluorophenylacetone in DME with 7.5 equiv. Et_3N.

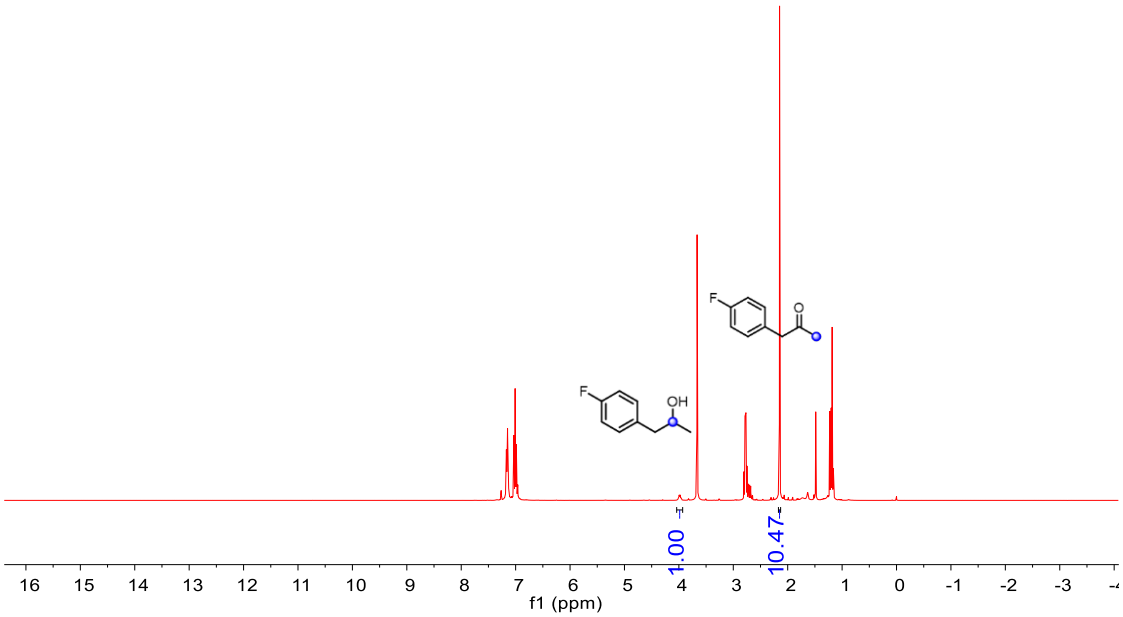

Figure S65. $^{1}H\{^{11}B\}$ NMR spectra in $CDCl_3$ for the reaction of $LiBH_4$ with 4-fluorophenylacetone in DME with 10 equiv. Et_3N.

6. Reference

(1) L. Tian and F. Chen, *J. Comput. Chem.* 2012, **33**, 58.

(2) D. C. Wigfield, *Tetrahedron*, 1979, **35**, 44.

(3) (a) H. C. Brown, S. Narasimhan and Y. M. Choi, *J. Org. Chem.*, 1982, **47**, 4702; (b) E. C. Ashby, F. R. Dobbs and H. P. Hopkins, *J. Am. Chem. Soc.*, 1973, **95**, 2823.

(4) X. Chen, X. Bao, B. Billet, S. G. Shore and J.-C. Zhao, *Chem. Eur. J.*, 2012, **18**, 1199.

(5) D. C. Wigfield, S. Feiner and F. W. Gowland, *Tetrahedron Letters*, 1976, **38**, 3377.

(6) D. C. Wigfield and Richard T. Pon, *J.C.S. CHEM. COMM.*, 1979, 910.

(7) R. K. Robinson and K. D. Jesus, *J. Chem. Educ.*, 1996, **73**, 264.

(8) D. C. Wigfield and D. J. Phelps, *Can. J. Chem.*, 1972, **50**, 38.

(9) E. R. Garrett and D. A. Lyttle, *J. Am. Chem. Soc.*, 1953, **75**, 6051.

(10) T. Lansbury and R. E. MacLeay, *J. Am. Chem. Soc.*, 1965, **87**, 831.

(11) J. A. Parry, and K. D. Warren, *J. Chem. Soc.*, 1965, 4049.

(12) D. C. Wigfield and F. W. Gowland, *J. Org. Chem.*, 1977, **42**, 110.

(13) G. G. Smith and R. P. Bayer**,** *Tetrahedron,* 1962, **18**, 323.

(14) D. C. Wigfield, *Tetrahedron*, 1979, **35**, 449.

(15) K. Bowden and M. Hardy, *Tetrahedron*, 1966, **22**, 1169.

(16) D. C. Wigfield and F. W. Gowland, *Tetrahedron Letters*, 1976, **38**, 337.

(17) P. Patel, S. Lingayat, N. Gulvi, P. Badani, *Chemical Physics*, 2018, **504**, 13.

(18) P. Song, M. Ruan, X. Sun, Y. Zhang, and W. Xu, *J. Phys. Chem. B*, 2014, **118**, 1022.